



UNIVERSITÀ DEGLI STUDI DI SALERNO



UNIVERSITÀ DEGLI STUDI DI SALERNO

Dipartimento di Farmacia

PhD Program

in **Drug Discovery and Development**

XXXI Cycle — Academic Year 2018/2019

PhD Thesis in

**The Winnie-APCmin as an Innovative Tool to
Investigate the Axis Between Inflammation and
Colorectal Cancer**

Candidate

Dott. *Marcello Chieppa*

Supervisor

Chiar.mo Prof. *Aldo Pinto*

PhD Program Coordinator: Prof. Dr. *Gianluca Sbardella*

INDEX

1. Introduction	
1.1 Cancer-related inflammation _____	Pag. 4
1.2 Inflammatory bowel diseases _____	Pag. 7
1.3 Animal models of CRC _____	Pag. 9
1.4 Anti-inflammatory effects of polyphenols _____	Pag. 11
2. Aims	
2.1 Creation of a murine model of inflammatory induced CRC__	Pag. 14
2.2 Nutritional strategies to suppress intestinal inflammation and Dysbiosis _____	Pag. 14
3. Methods	
3.01 Mice _____	Pag. 15
3.02 Histology _____	Pag. 17
3.03 RNA extraction and qPCR analysis _____	Pag. 17
3.04 Bacterial microbiome metagenomics _____	Pag. 18
3.05 Generation and culture of murine DCs _____	Pag. 19
3.06 Purification of OBs _____	Pag. 20
3.07 Quercetin and piperine encapsulation into ROBAs _____	Pag. 21
3.08 Microarray gene expression analysis of ROBAs-QP-treated DCs_	Pag. 22
3.09 Small interfering RNA (siRNA) _____	Pag. 23
3.10 ELISA _____	Pag. 24
3.11 Iron staining _____	Pag. 24
3.12 Western blotting _____	Pag. 24
3.13 Tomato-enriched diet administration _____	Pag. 25
3.14 Cytofluorimetric Analysis _____	Pag. 26
3.15 Statistical Analysis _____	Pag. 27
4. Results	
4.01: Winnie-APC ^{Min} murine line pathological features. _____	Pag. 29
4.02: Winnie-APC ^{Min} mice develop dysplastic lesions. _____	Pag. 31
4.03: 5 week-old Winnie-APC ^{Min} mice gene expression. _____	Pag. 33
4.04: Metagenomic analysis in 4 week-old Winnie-APC ^{Min} mice. ____	Pag. 35
4.05: Quercetin induces Slpi expression in LPS-activated BMDCs ____	Pag. 37
4.06: Quercetin reduces TNF α secretion by up-regulating Slpi _____	Pag. 39
4.07: Quercetin effects are lost enriching the culture media with iron_	Pag. 41
4.08: Gut Microbiota Respond to the Iron Starvation _____	Pag. 44
4.09: Effects of nutritional intervention in Winnie mice _____	Pag. 47
4.10: IL-17A Reduction in CD4+ Mesenteric Lymph Node (MLN) T Cells Treated with a Bronze Tomato Diet _____	Pag. 48
4.11: Bronze Tomato Diet Molecular Signature _____	Pag. 50
4.12: Dysbiotic Intestinal Microbiota Communities Changed Following Two Weeks on a Bronze Tomato Diet in Winnie Mice _____	Pag. 51

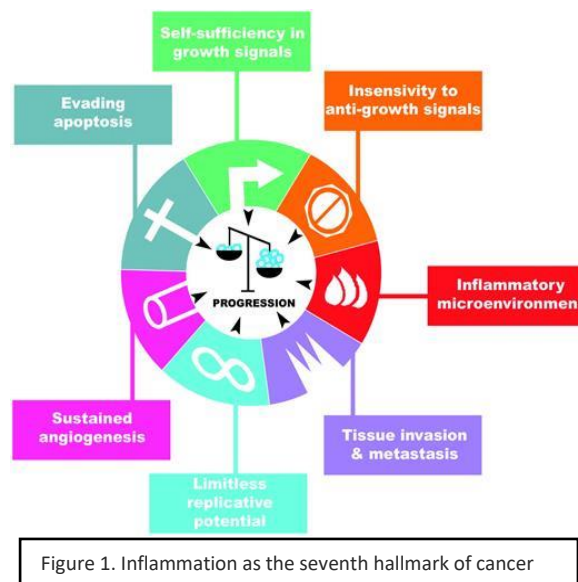
5.	Conclusions _____	Pag. 53
6.	References _____	Pag. 56

1. INTRODUCTION

1.1 Cancer-related inflammation

Worldwide occurrence of autoimmune diseases and cancer is increased, this is particularly clear in more developed countries [1]. Several environmental factors, including pollution and increased average age, may play a role and partially explain this observation, but the concurrence of inflammation and cancer seems to be connected and not independent. Similarly,

but from the opposite direction, the introduction of non-steroidal anti-inflammatory drugs to protect for chronic inflammatory syndromes was able to protect patients from the increased risks of



cancer development [2]. Epidemiological studies demonstrated that chronic inflammation predisposes to different forms of cancer, thus cancer-related inflammation, was recently included as the seventh hallmark of cancer [3].

Before the introduction of effective therapeutic options, inflammatory bowel diseases (IBDs) were associated with increased risk of developing colorectal cancer (CRC). IBDs are chronic inflammation of

the gut that include Crohn Disease (CD) and Ulcerative Colitis (UC). IBDs are multifactorial disorders characterized by, abdominal pain, diarrhea and rectal bleeding [4].

In patients with long-established IBD, the risk of developing colon cancer is increased, thus CRC was the perfect target to study the axis between chronic inflammation and cancer.

CRC was first recognized as a complication of ulcerative colitis (UC) by Crohn and Rosenberg in 1925. Although CRC in UC patients only accounts for 1% of all cases of CRC seen in the general population, it accounts for one sixth of all deaths in UC patients. For this reason, it deserves a great attention. Since 1925, numerous epidemiological studies have confirmed an increased risk of CRC for UC patients in the first decade after an UC diagnosis [4]. More recent studies have reported that this risk at later stages of UC has decreased markedly over time and no longer exceeds that of the general population. Although the risk in adults continues to be a matter of debate, the general consensus from all studies agrees with the view that CRC risk is highest in patients who are diagnosed with UC during childhood, adolescence or young adulthood, especially in male patients. The reduced risk of CRC incidence in older UC patients over time reflects the results of improvements in the therapy of IBD patients and the introduction of routine endoscopic screening [5].

Corticosteroids and especially, 5-ASA and thiopurines are used as chemopreventive agents due to their ability to inhibit, delay or reverse CRC in UC. Recently, biologic agents have been introduced for the

induction and the maintenance of therapy in IBD patients. In Europe, the approved agent is infliximab, a monoclonal antibody that blocks tumor necrosis factor α (TNF α), one of the most important molecules involved in the pathogenesis of IBD.

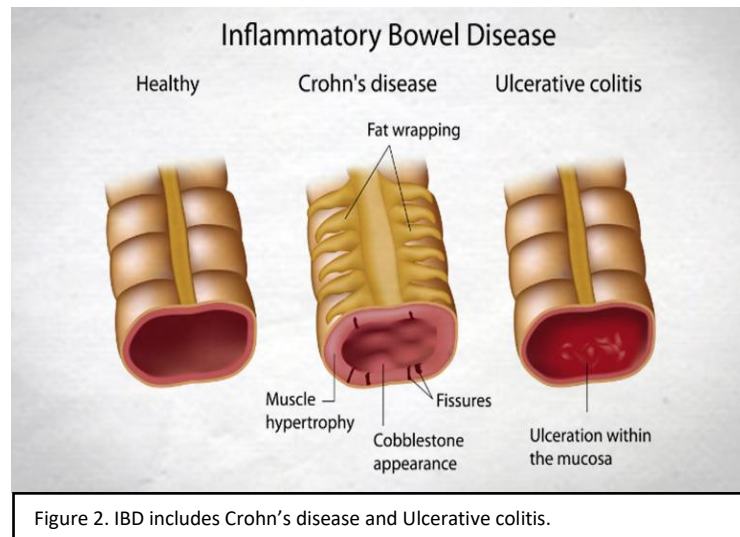
However, conflicting reports exist concerning the relationship between infliximab and an increased risk of CRC and other forms of cancer in IBD patients receiving such therapy. While infliximab treatment has been associated with the development of carcinoid tumor, signet ring cell carcinoma of the bowel, breast cancer, lung cancer, and colorectal cancer, however, in other cases there was no significantly increased risk of cancer by TNF α antagonist exposure [6]. It is tempting to speculate that, due to the recent introduction of biological agents into the clinical practice, long-term observational studies of these treatment sequelae are needed. Furthermore, these divergent data are reported to be due to perhaps the intrinsic dual nature of the immunomodulatory drugs that both induce a decreased immunosurveillance, thereby providing advantages for oncogenic viruses, and exert a direct oncogenic effect for certain immunosuppressive drugs. These effects are not limited to the intestinal epithelium; in fact, cases of extra-intestinal neoplasia, such as lymphoproliferative disorders, skin and uterine cervical cancer have been reported in IBD patients under immunosuppressive treatment. Thus, immunosuppression and inflammation are the two main drivers of IBD-related carcinogenesis. The challenge is that these two mechanisms may be interlinked, particularly in the intestinal tissues.

The dual nature of TNF α activity is responsible for its paradoxical anti- and protumor activity depending on cell type, environment, dose, and other factors. On one hand, TNF α exerts its anti-tumoral potential by its interaction with death domain containing proteins and caspases that induce apoptosis. On the other hand, TNF α has a pro-tumoral activity resulting from the activation of NF- κ B and mitogen-activated protein kinase pathways, which are in turn associated with inflammation and carcinogenesis [7].

1.2 Inflammatory bowel diseases

Inflammatory bowel diseases (IBD) include Crohn's Disease (CD) and Ulcerative Colitis (UC), which are both chronic relapsing inflammatory disorders of the gastro-intestinal tract [8].

The mucosal immune system is dynamically regulated to a state of tolerance to luminal antigens including commensal



bacteria and food derived antigens. However, breaches of mucosal immune tolerance can occur due to both environmental and genetic

factors resulting in perturbed intestinal homeostasis. Several different events can trigger inflammatory responses that may result in chronic inflammation and pathological changes associated with IBD. A common ground for this multifactorial disorder is an increased production of diverse panel of cytokines, [9] some of which are pro-inflammatory and hence targets for therapeutic blockade.

As aforementioned, clinical investigations have led to the discovery of

anti-TNF α
 monoclonal
 antibodies
 (Infliximab
 and others)
 which has

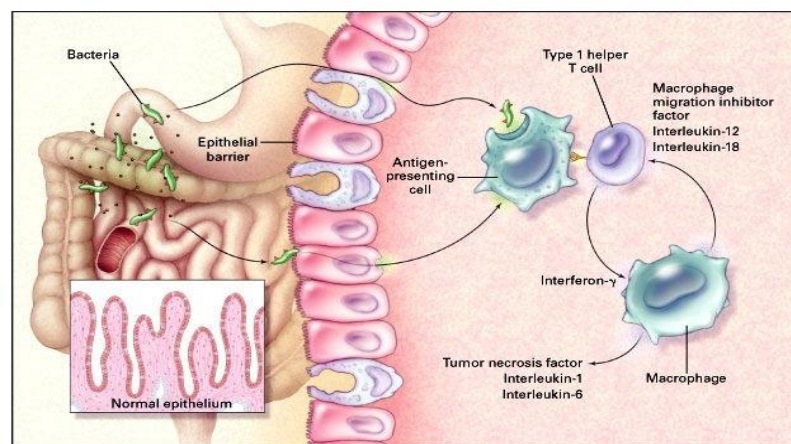


Figure 3. Perturbed intestinal homeostasis and cytokine production in IBD patients [9].

dramatically changed the medical approach to IBD. Similar to CD, a subgroup of UC patients also exhibit increased TNF α levels in the colon. In fact, Braegger et al. reported the presence of TNF α in stool samples in such UC patients [10]. Animal models have significantly contributed to the elucidation of the pathological mechanisms of IBD and to the validation of immunological targets for IBD treatment [11].

1.3 Animal models of CRC

To dissect the intricate relationship between inflammation and increased cancer risks we decided to take advantage of the well consolidated murine models of genetic predisposition leading to CRC (APC^{min} mice) and a low grade, spontaneous and progressive UC model (Winnie).

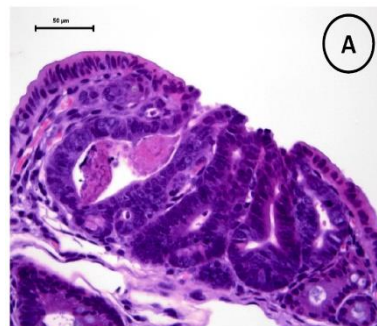


Figure 4. H&E stain for histopathology of a murine colonic tumor.

We created a new murine model of colitis-associated cancer, the Winnie-APC^{Min} model [12].

The APC^{min} murine model is among the most frequently used model to study colorectal cancer (CRC), even if conventional protocols require the administration of dextran sodium sulfate (DSS) as inflammatory insult to develop CRC in a relatively short time. DSS specifically acts on the

intestinal epithelium integrity to induce an acute inflammation characterized by multiple events that poorly represent the cascade of events that characterize the human ulcerative colitis [13-15].

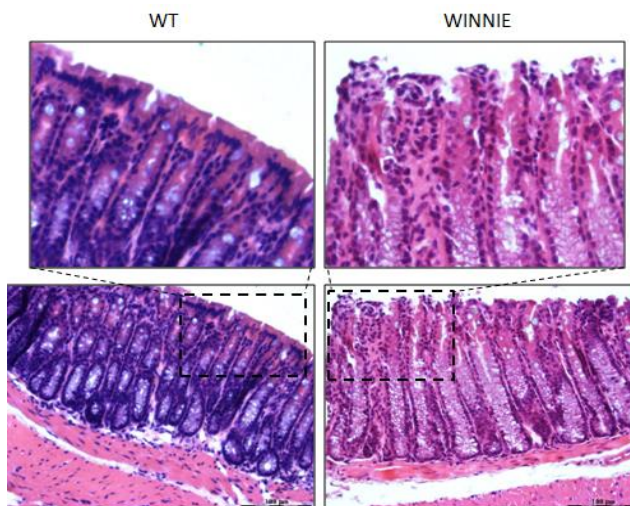


Figure 5. H&E stain for histopathology of Winnie mice [Liso et al. Under Revision].

To overcome this bias and create a reliable model of inflammatory induced CRC, we crossed APC^{min} with Winnie mice. *Winnie* colitis is due to a missense mutation in the *Muc2* mucin gene resulting in spontaneous distal colitis developing as early as 5 weeks of age [16]. This intestinal epithelial defect conferring endoplasmic reticulum (ER) stress results in inflammation involving both innate and adaptive immunity. In the *Winnie* mouse the colonic pathology is predominantly mediated by the dysregulation of numerous cytokines, including elevated TNF α similar to human UC where the intestinal inflammation is most severe in the distal colon and the disease severity increases with age.

The risk of neoplastic progression in IBD is multi-factorial. This heterogeneity may at least in part be due to differences in genetic susceptibility, which may act in combination with various environmental factors including diet and intestinal microbial community [17]. In particular, the intestinal microbiota has recently acquired a great interest in the context of inflammation and carcinogenesis [18]. Murine models allow investigation of the intestinal microbiota and CRC-associated dysbiosis.

For this reason, in parallel with the creation of a Winnie-APC^{min} colony, we investigated the possibility to use nutritional strategies to reduce the intestinal inflammation and prevent the associated intestinal dysbiosis. As dysbiosis has recently been suggested as the cause of disease recurrence for patient that achieved UC clinical remission, nutritional

strategies may prevent dysbiosis and, consequently, remove one of the inflammatory insult required for CRC development.

1.4 Anti-inflammatory effects of polyphenols

A major field of investigation of our laboratory is characterization of the anti-inflammatory properties of plant-derived polyphenols. Dietary polyphenols are associated with a wide range of health benefits, protecting against chronic diseases and promoting healthy aging. Dietary polyphenols offer a complementary approach to the treatment of inflammatory bowel diseases (IBD), a group of common chronic intestinal inflammation syndromes for which there is no cure. Several studies have described the beneficial effects of plant-derived

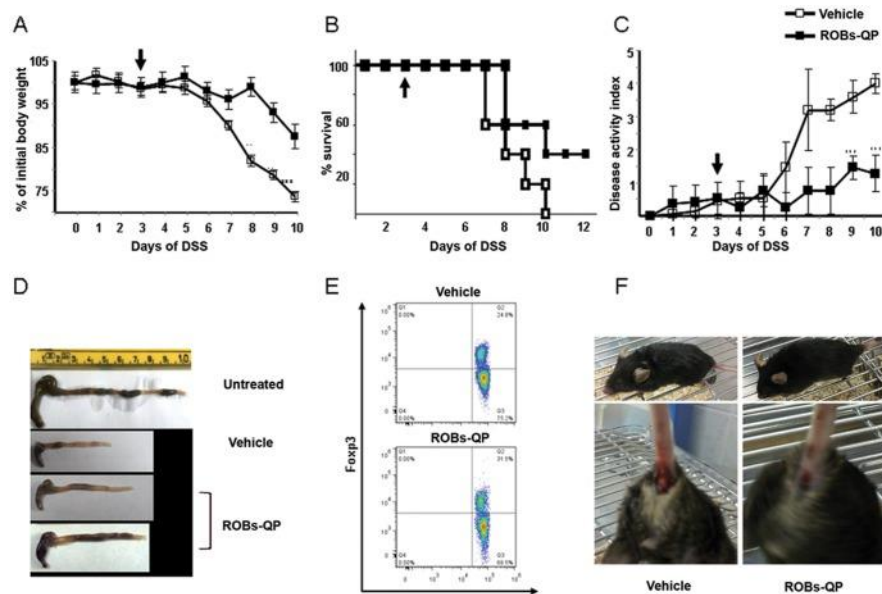


Figure 6. Intraperitoneal administration of ROBs ameliorates 2% DSS-mediated acute colitis [20].

polyphenols as natural ligands that are able to reduce inflammation, with some inhibiting production of TNF α from cell lines of different

origins in both in vitro and in vivo models [19, 20]. In our laboratory we previously compared numerous polyphenols and identified quercetin as one of the most potent suppressor of the inflammatory response [21]. Quercetin, similarly to many other phytochemicals, is a hydrophobic compound characterized by low solubility in water and consequent low bioavailability. These major limitations can be bypassed by developing efficient delivery systems that have the ability to protect, as well as release, polyphenols at the appropriate site of action. A wide variety of new delivery systems has been proposed, including liposomes, nanoparticles, and nanoemulsions [22]. Among these, plant oil bodies (OBs) represent a convenient and feasible option to achieve the aforementioned goals. OBs are lipid storage vesicles that are naturally found in plant seeds. Isolated OBs are remarkably stable due to the steric hindrance and electro-negative repulsion provided by surface proteins of the organelles [23, 24]. Reconstituted oil bodies (ROBs), as well as native OBs, have been previously reported as useful vehicles for the stabilization of curcumin and previously used by our research group to demonstrate the ability of polyphenol administration to suppress dendritic cells inflammatory pathway [21].

Another strategy recently-developed strategy to administrate hi-doses of stable polyphenols was developed by the research group of Prof. Cathie Martin [25]. In 2008 they created a tomatoe line engineer to accumulate anthocyanin at concentrations comparable to the anthocyanin levels



Figure 7. Wild type versus purple tomatoes [21].

found in blackberries and blueberries. Possibly due to the polyphenol anti-inflammatory abilities and the previously unknown effect to the intestinal microbial communities, the administration of these tomato fruit to cancer-susceptible $Trp53^{-/-}$ mice resulted in a significant extension of life span [25].

We recently obtained new lines of dried tomatoes fruit enriched in polyphenols to evaluate possibility to use nutritional regimes enriched in polyphenols to suppress the chronic intestinal inflammation and protect from intestinal dysbiosis.

2. Aims

2.1 Creation of a murine model of inflammatory induced CRC

The development of murine models to study CRC development and progression has been crucial to better understand the disease and to develop new therapies. The most frequently used murine models of tumor development combine the administration of the carcinogen agent azoxymethane or the genetic predisposition APC^{min} with various agents promoting colonic injury such as DSS, oxazolone or enterotoxigenic bacteria *Bacteroides fragilis* [13, 26-28]. The aim of the study was to create a new murine line of spontaneous inflammatory-induced colorectal cancer combining the genetic predisposition APC^{min} with the mutation in the Muc2 gene that results in ER stress and spontaneous mild and progressive UC.

In particular, we aim to:

- Create and establish the Winnie-APC^{min} colony.
- Characterize the development of neoplastic lesion in the intestine of this new model.
- Characterize the intestinal molecular fingerprint of the new murine lines.
- Characterize the intestinal microbiota of the new murine lines.

2.2 Nutritional strategies to suppress intestinal inflammation and dysbiosis

Together with numerous other research group, we already reported the anti-inflammatory potential of numerous natural bio-active compounds as potential candidate for prevention and treatment of the intestinal inflammatory response. [21, 29, 30] Despite evidences for the biological effects of these phytonutrients being reported, knowledge of the underlying molecular mechanisms activated upon polyphenols treatment remain poorly understood. A second parallel aim of the study

was to explore the possibility to prevent intestinal inflammation using nutritional derived bioactive compounds. To achieve this goal we studied the effects of quercetin administration to in-vitro cultured dendritic cells that are the most powerful antigen presenting cells. Furthermore we tested the effects of polyphenol enriched diet to the relative abundance of intestinal microbial species.

In particular, we aim to:

- Identify quercetin induced molecular mediators suppressing the inflammatory response.
- Characterize the mechanism of the quercetin induced inflammatory suppression.
- Evaluate the effects of nutritional intervention in the murine model of UC (Winnie).

3. METHODS

3.01 Mice

The new murine transgenic line Winnie-APC^{Min} was created by breeding Winnie mice, a murine line established from Dr. Eri's group at the University of Tasmania, with APC^{Min} mice murine line on a C57BL/6J background. WT, APC^{Min} and secretory leukocyte protease inhibitor (SLPI) knockout mice murine lines were purchased from Jackson Laboratories (C57BL/6J, Stock No. 000664, C57BL/6J-ApcMin/J, Stock No. 002020, B6; 129-Slpi^{tm1Smw}/J, Stock No: 010926 respectively) (Bar Harbor, ME, USA). All animal experiments were carried out in accordance with EU Directive n.63/2010 enforced by Italian D.L. n.26/2014, and approved by the Committee on the Ethics of Animal

Experiments of Ministero della Salute – Direzione Generale Sanità Animale (768/2015-PR 27/07/2015) and the official RBM veterinarian. Animals were sacrificed if found in severe clinical condition in order to avoid undue suffering. Winnie-APCMin mice and their parental lines were sacrificed at 5 weeks and colon was explanted to evaluate the clinical severity of colitis. C57BL/6 and Winnie mice were treated with different diet and sacrificed after two weeks of treatment. For the latter, mice weight, pellet consumption and drinking water were monitored on a daily basis. Each group of mice received a different diet. Freeze-dried tomato was supplemented by addition to a standard rodent diet (4RF18) at 1% (tomato based-diets). Groups of mice were fed with the different tomato supplemented diets for two weeks. Body weight, stool consistency and rectal bleeding were recorded. Mice were sacrificed at day 14, and colon and mesenteric lymph node (MLN) tissues were explanted to evaluate the clinical severity of colitis. Colon length and weight were measured as indicators of colonic inflammation. The colon/body weight indices were calculated as the ratio of the colon wet weight and the total body weight (BW), and as the ratio of the colon length and the total BW of each mouse. Genotyping was performed by PCR (APCMin) and qPCR (Winnie) from 5mm tail tissue obtained from 4-week old mice, DNA was extracted using DNeasy® kit purchased by QIAGEN and following manufacturer's instructions. For APCMin we followed the official PCR protocol described by the Jackson Laboratory (https://www2.jax.org/protocolsdb/f?p=116:2:0::NO:2:P2_MASTER_PROTOCOL_ID,P2_JRS_CODE:15431,002020); for Winnie mice we

performed a single nucleotide polymorphisms (SNP) genotyping analysis using a custom TaqMan® Assay (AHCSX8U) to discriminate for the presence of a point mutation on the Mucin 2 gene by a real-time PCR reaction.

3.02 Histology

Tissue sections from large intestine were fixed in 10% buffered formalin, dehydrated and paraffin embedded. Based on the major intestinal axis, the samples had a length variable between 0.5 cm and 1.5 cm and span of all the colonic wall. We evaluated a mucosal area between 7.5 mm² and 22.5 mm² wide with a mean measure of 15 mm². 3µm thick-sections from proximal, medial and distal colon were stained with H&E following standard protocols. Colonic tissue sections were evaluated for inflammatory features and neoplasia. Periodic acid–Schiff (PAS) staining on distal colon sections was performed to identify mucins. Observations and imaging were performed with Nikon Eclipse Ti2.

3.03 RNA extraction and qPCR analysis

Total RNA was isolated from the medial part of the large intestine or bone marrow derived dendritic cells (BMDCs). The RNA was extracted using TRIzol® (Thermo Fisher Scientific, MA, USA) according to manufacturer's instructions and reverse transcribed with I Script Reverse Transcription Supermix (BioRad Laboratories, CA, USA). 500ng

of total RNA was reverse transcribed with the High Capacity cDNA Reverse Transcription kit (Thermo Fisher Scientific, MA, USA) by using random primers for cDNA synthesis. Gene expression of Il1 β , Ifn γ , Il12, Il10, Il4, TNF α , Slpi, Hmox1 and Gapdh was performed with TaqMan Gene Expression Assays (Thermo Fisher Scientific MA, USA) murine probes: Mm00434228_m1, Mm01168134_m1, Mm01288989_m1, Mm00439614_m1, Mm00445259_m1, Mm00443258_m1, Mm00441530_g1, Mm01254822_m1, Mm99999915_g1, respectively. Tier-based gene expression analysis was performed by using Colonic neoplasms Tier 1 M96 (Cat.#100-36551, Biorad, CA, USA). Real-time PCR was performed on CFX96 System (Biorad, Hercules, CA, USA). The expression of all target genes was calculated relative to Gapdh expression using $\Delta\Delta C_t$ method.

3.04 Bacterial microbiome metagenomics

Total genomic bacterial DNA was isolated from frozen stool samples of 4-, 8- and 16-week old WT and Winnie mice (4 samples/genotype for each timing) using the QIAamp® Fast DNA Stool Mini Kit (QIAGEN, Hilden, Germany), according to manufacturer's instructions.

16S metagenetics were carried out at Genomix4life (spin-off of the University of Salerno, Italy) by using the Illumina MiSeq platform. The V3-V4 region of the 16S rRNA gene for analysis of diversity inside the domains of Bacteria was amplified.¹⁸ PCR and sequencing analyses were carried out according to the protocol of Genomix4life. Quality

control (QC) and taxonomic assignments were undertaken according to the QIIME and the Ribosomal Database Project Bayesian classifier in combination with a set of custom designed informatics pipelines implemented by Genomix4life for analyses of microbial communities. Taxonomic attribution was carried out using the BLAST search in the NCBI 16S ribosomal RNA sequences database.¹⁹ The percentage of each bacterial OTU was analysed individually for each sample, providing relative abundance information among the samples based on the relative numbers of reads within each.²⁰ Alpha-diversity indexes were evaluated using the number of OTUs, Chao1 species richness and the Shannon index. Alpha diversity was calculated using Qiime.²¹⁻²²

3.05 Generation and culture of murine DCs

DCs were harvested from murine bone marrow (BM). Briefly, BMs from the tibiae and femurs of 6- to 8-week-old male C57BL/6 and Sipi-KO mice were flushed with 0.5mM EDTA (Thermo Fisher Scientific, MA, USA), and depleted of red blood cells with ACK lysing buffer (Thermo Fisher Scientific, MA, USA). BMDCs were plated in a 10 ml dish (1×10^6 cells/mL) in RPMI 1640 (Thermo Fisher Scientific, MA, USA) supplemented with 10% heat-inactivated fetal bovine serum (FBS, Thermo Fisher Scientific, MA, USA), 100 U/mL penicillin (Thermo Fisher Scientific, MA, USA), 100 mg/mL streptomycin (Thermo Fisher Scientific, MA, USA), 25 µg/mL rmGM-CSF (Miltenyi Biotec, Bergisch Gladbach, GER), and 25 µg/mL rmIL-4 (Miltenyi Biotec, Bergisch

Gladbach, GER) at 37°C in a humidified 5% CO₂ atmosphere. On day 5 BMDCs were harvested, restimulated with new growth factors and plated at 1x10⁶ cells/mL on 24-well culture plate. BMDCs were treated with 25µM of quercetin from Sigma (Sigma-Aldrich, St Louis, MO, USA) on day 5 and day 7. On day 8 BMDCs were stimulated with 1 µg/mL of LPS (L6143, Sigma-Aldrich, St Louis, MO, USA) for 24 hours. To evaluate the iron-induced inflammatory cytokine secretion, differentiating cells (at day 7) were treated with quercetin (Sigma-Aldrich, St Louis, MO, USA) or OH-piridone used as control chelator. Immediately after, FeCl₃ (Sigma-Aldrich, St Louis, MO, USA) and Ascorbic Acid for 24 hours were added in the culture media. On day 8 BMDCs were stimulated with 1 µg/mL of LPS (Sigma-Aldrich, St Louis, MO, USA) for 24 hours. For mRNA expression differentiating cells were treated with quercetin on day 5 and day 7. On day 8 BMDCs were stimulated with 1 µg/mL of LPS (Sigma-Aldrich, St Louis, MO, USA) for 6 hours.

3.06 Purification of OBs

OBs were extracted from almond seeds. OB purification was carried out by a two-layer flotation procedure as previously reported [31], and a further purification step was performed consisting of two sequential washings with 2.0 M NaCl. OBs were finally resuspended in 150 mM Tris-HCl, pH 7.5, containing 0.6 M sucrose.

3.07 Quercetin and piperine encapsulation into ROBs

Quercetin and piperine were encapsulated into the ROBs using the above reported protocol [31] with few modifications. Natural OBs were resuspended in 150 mM TRIS-HCl pH 7.5, containing 0.5 M sucrose, 1 mM EDTA, 10 mM KCl, 1 mM MgCl₂, 5 mM ascorbic acid (buffer A) and twice extracted with chloroform : methanol (2:1), in order to separate PLs and proteins from TAGs. After centrifugation at 1000 g for 5 minutes, the upper phase was extracted with five volumes of diethyl ether anhydrous (to recover TAGs). All the recovered fractions were dried by a rotavapor. ROB reconstitution mixture consisted of the whole chloroform-methanol phase (PLs) with a quercetin (or piperine)/TAGs ratio of 1/250 starting from 2 mg of each phytochemical. The final volume was adjusted to 3 ml by the addition of buffer A. Samples were sonicated by a Brandson digital Sonifier 250-D at an amplitude of 40% and a cycle of 30 seconds pulse on and 30 seconds off for three times. After sonication, samples were centrifuged at 2000 g for 10 minutes and ROBs containing quercetin or piperine were recovered from the top of the centrifuge-tubes. HPLC analysis was carried out extracting the encapsulated phytochemicals using 2 volumes of ultrapure water, 2 volumes of methyl-butyl-ether, and 1 volume of methanol. After centrifugation at 1000 g for 5 minutes, the methyl-butyl-ether phase was recovered, dried (rotavapor), and resuspended into 50% ethanol. Quercetin was quantified by reverse phase-HPLC using the method described above [32] onto a 1100 Agilent work chromatographic station

equipped with a photodiodes array UV-Vis detection system. The elution profile was monitored at 370 nm. Quercetin, purchased from Sigma-Aldrich, was used as standard.

3.08 Microarray gene expression analysis of ROBS-QP-treated DCs

BMDCs were isolated and cultured as described. On day 5 and day 7 BMDCs were treated with ROBS-QP (25 μ M). LPS was administered [1 μ g/mL] at day 8 and 6 h later BMDCs were harvested. Total RNA was isolated with QIAzol (Qiagen, Hilden, GER) and treated with DNAase1 (Ambion). RNA integrity was assessed using the BioRad Experion System (BioRad Laboratories). RNA was amplified using the Illumina TotalPrep RNA Amplification kit (Ambion). The quantity and quality of biotin-UTP incorporated

cRNA was also assessed using the BioRad Experion System as previously described. Whole-genome gene expression experiments were conducted using MouseRef-8 v2.0 Expression Bead-Chips (direct hybridization assay) on the Illumina iScan microarray platform (Illumina). Data were processed through specific algorithms of filtration and cleaning of the signal of the Illumina Genome Studio Software (Cut off: detection p-value < 0.005; AVG signal < 100). Final output consisted of fluorescence intensity of each probe (AVG signal), representing the expression levels of each gene after quantile normalization. All the genes differentially expressed ("Differential Expression Analysis" with the

“Illuminacustom error model” and with false Discovery Rate to adjust the p-value) between groups were analyzed using the Core Analysis function of Ingenuity Pathway Analysis (Ingenuity System Inc., Redwood, CA, USA) to identify biological functions, pathways, and networks.

3.09 Small interfering RNA (siRNA)

siRNA transfection was performed in BMDCs culture from WT mice obtained as described before. Cells were cultured at 1×10^6 in a 12-well plate and the transfection was carried out at day 4 using Lipofectamine 3000 (Thermo Fisher Scientific, MA, USA) in accordance with manufacturer's procedure. siRNA for Slpi were purchased from Thermo Fisher Scientific (s202008) and used at a final concentration of 40 pmol. In transfection experiments a mock-transfection control was performed by putting cells through the transfection procedure without adding siRNA. The Silencer Select Negative Control siRNA (4390843, Thermo Fisher Scientific, MA, USA) and Silencer® Select GAPDH Positive Control siRNA (4390849, Thermo Fisher Scientific, MA, USA) were used as negative control and positive control, respectively, for the setup of siRNA transfection. Each transfection experiment was done in triplicate. On day 5, cells were treated with 25 μ M of quercetin and the day later cells were stimulated with 1 μ g/ml of LPS. After 24 hours, cells were

lysed with TRIzol® (Thermo Fisher Scientific, MA, USA) and used for total RNA extraction.

3.10 ELISA

Cell culture supernatants were analyzed for IL-6, IL-12p70 and TNF α release in triplicate, using an ELISA kit (R&D Systems, Minneapolis, MN, USA) following manufacturer' instructions.

3.11 Iron staining

BMDCs, were plated for 24h into Glass Bottom Cell Culture Dishes (MatTek corporation P35G-1.5-14.C), and treated with and without quercetin and FeCl₃ (day 7). Following BMDCs cultures were exposed to 1 μ g/mL of LPS and stained with The Iron Stain Kit (GENTAUR Molecular Products; IRN-2 Belgium) for the determination ferric iron deposits in tissue samples. This product is based on the Prussian Blue reaction in which ionic iron reacts with acid ferrocyanide producing a blue color. BMDCs were fixed in 1% paraformaldehyde and then stained following manufacturer instructions.

3.12 Western blotting

The amount of Hmox1, after stimulation of quercetin, was determined by Western blot analysis. Total protein extract were prepared with lysis

buffer containing 150 mM NaCl, 50 mM Tris-HCl (pH 8), 1% NonidetP-40, 0.1% sodium deoxycholate, 0.1% SDS, plus proteinase inhibitors. The protein concentration was determined by the Bradford assay (BioRad, CA, USA). 30 µg of each protein lysate was separated on a 10% SDS-PAGE and transferred to polyvinylidene difluoride (PVDF) membrane (Millipore, MA, USA). The membranes were incubated in 5% non-fat milk powder diluted in PBS containing 0.1% Tween-20 (T-PBS) for 2h at room temperature (RT) and probed with a rabbit polyclonal anti-Hmox1 antibody (PA5-27338 ThermoFischer scientific MA, USA) in blocking buffer overnight at 4°C at a final dilution of 1:1000. Finally, membranes were incubated with secondary antibody of horseradish peroxidase conjugated goat anti-rabbit IgG (Santa Cruz Biotechnology, CA, USA) at a final dilution of 1:5000. Immunocomplexes were detected with the ECL method (GE Healthcare, Little Chalfont, UK). The same membranes were stripped and re-probed with anti- α -tubulin monoclonal antibody (Santa Cruz Biotechnology) at a final dilution of 1:2000. Images of Western-blot were acquired and quantified using a ChemiDoc MP (BioRad, CA, USA) apparatus. Ratio between intensities of Hmox1 and α -tubulin bands was used to normalize Hmox1 in each sample.

3.13 Tomato-enriched diet administration.

The Bronze tomato line (E8:MYB12, E8:Del/Ros, 35S:StSy) was developed as previously described [34]. Freeze-dried tomato was supplemented by addition to a standard rodent diet (4RF18) at 1%

(tomato based-diets). Mice, pellet consumption and drinking water were monitored on a daily basis.

Sex- and weight-matched mice were divided in 5 groups (5 WT mice each). Each group of mice received a different diet. Groups of mice were fed with the different tomato supplemented diets for two weeks. Stools were collected and stored at -80°C.

For the intervention experimental setup, sex- and weight-matched mice were divided into four groups (four mice each). Groups of mice (WT and Winnie) were fed with the different tomato supplemented diets for two weeks. Mice were sacrificed at day 14, and colon and mesenteric lymph node (MLN) tissues were explanted to evaluate the clinical severity of colitis. Colon length was measured as an indicator of colonic inflammation. The colon/body weight indices were calculated as the ratio of the colon wet weight and the total body weight (BW), and as the ratio of the colon length and the total BW of each mouse. Body weight, occult and rectal bleeding and stool consistency were monitored daily. Disease activity index (DAI) was determined by scoring changes in body weight, occult blood and gross bleeding.

3.14 Cytofluorimetric Analysis

FoxP3 staining: Mesenteric lymph nodes (MLNs) were isolated from mice fed with tomato (Control or Bronze)-enriched food. MLNs were passed through a 30 µm cell strainer (Miltenyi Biotec, Bergisch

Gladbach, Germany) to obtain a single cell suspension and then washed with DPBS (Gibco, Waltham, MA, USA) + 0.5% bovine serum albumin (BSA, Sigma-Aldrich, St. Louis, MO, USA). Single cell suspensions were stained with CD4-FITC and CD25-PE (Miltenyi Biotec, Bergisch Gladbach, Germany). Cells were then permeabilized with Foxp3 Fixation/Permeabilization Kit (eBioscience, San Diego, CA, USA) and subsequently washed with PERM Buffer (eBioscience, San Diego, CA, USA). Finally, cells were stained with Foxp3-APC (Miltenyi Biotec, Bergisch Gladbach, Germany), according to the manufacturer's instructions. Flow Cytometer acquisition was performed using NAVIOS (Beckman Coulter, Brea, CA, USA).

T cell Intracellular Staining: T cells from MLNs of mice fed with tomato (Control or Bronze)-enriched food were cultured with a 500X Cell Stimulation Cocktail (eBioscience, San Diego, CA, USA) for 12 h, washed with DPBS + 0.5% BSA and stained with CD4-APC-Vio700 (Miltenyi Biotec, Bergisch Gladbach, Germany). After washing, cells were then permeabilized with BD CytoFix/CytoPerm® Fixation/Permeabilization Kit® (BD Biosciences, Franklin Lakes, NJ, USA), washed with PERM Buffer, and stained with: IL-17A-FITC, TNF α -PE and IFN γ -APC according to manufacturer's instructions (Miltenyi Biotec, Bergisch Gladbach, Germany). Flow Cytometer data analysis was performed using NAVIOS (Beckman Coulter).

3.15 Statistical Analysis

All data were expressed as the means \pm SEM. All results were obtained from three consecutive and independent experiments. Metagenomic data (Unifrac distance metric and taxonomic abundance) were analyzed by Principal Component Analysis (PCA)²³ using a statistical software Statistica for Windows (Statistica 6.0 for Windows 1998, StatSoft, Vigonza, Italia). Permut-MatrixEN software was used to identify clusters at the level of the mouse groups and taxa.²⁴ Statistical analysis of the relative abundances of microbial genera was based on Duncan's Multiple Range test, with a significance level of $p \leq 0.05$. Finally, unless specifically described, other data and group differences were analyzed and compared by paired or unpaired, two-tailed Student's t-tests.

Cell biology data statistical significance was evaluated using two-tailed Student's t test, One Way ANOVA followed by Tukey's multiple comparison as post test and the 2way-ANOVA test using the Bonferroni as a post-test for the grouped analysis. Results were considered statistically significant at $p < 0.05$.

4. RESULTS

The Winnie-APC^{min} model

We believed that the Winnie-APC^{min} could become an animal model that better resembles the chronic inflammatory insult recently included as a leading factor for cancer development (including CRC) [3]. During these past 3 years, we have successfully established the Winnie-APC^{min} colony and carefully characterized the development of neoplastic lesion in the intestine of this new model compared with all the parental lines. Morphological, molecular and immunological results of this study demonstrate that the Winnie-APC^{min} model is a unique model that could be a perfect to address the role of inflammation as a trigger for CRC in genetically predispose patients. In fact, the intestinal epithelium of Winnie- APC^{min} mice develops dysplastic lesions at early time points with a progression over time that confirm a multi-step process for CRC carcinogenesis.

4.01: Winnie-APC^{Min} murine line pathological features.

To generate a mouse model that reflect the increased intestinal cancer risk of UC patients we used a mice breeding strategy counted on double heterozygote mutations (on Muc2 and APC^{Min} genes) for males and single heterozygote mutation (Muc2) for females (Figure 8A). This strategy allowed obtaining colitis associated-CRC (CA-CRC) model (Winnie-APC^{Min}) together with all the parental strains (WT, Winnie and APC^{Min} mice) from the same couple. Using this strategy, it was possible

to collect data related to strains survival and inflammatory features comparing genetically different offspring obtained from the same

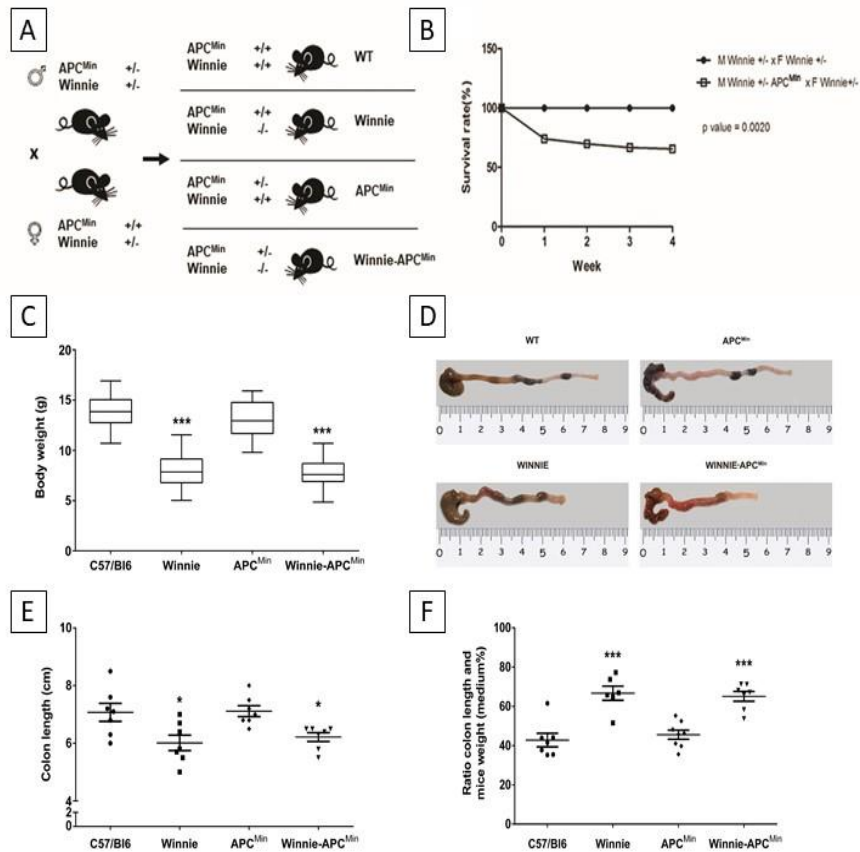


Figure 8: Creation and characterization of the Winnie-APC^{Min} murine model. (A) Breeding strategy used to obtain Winnie-APC^{Min} mice and the parental lines from the same breeders. (B) Impact of APC^{Min} mutation on survival rate in the breeding scheme of Winnie mice. (C) Body weight analysis of 4-week-old mice from different genotypes. Representative images of colons (D) and data analysis of colon length (E) and colon length adjusted to the body weight (F) for Winnie-APC^{Min} mice and control lines. C-F: 7 animals/group. *p<0.05, ***p<0.001 compared to WT mice.

breeders. If compared with the breeding strategy used to obtain Winnie mice, when the APC^{Min} mutation was introduced in the breeding scheme there was a reduction in the survival rate (28.6% versus 0.8%, Figure 8B). Similarly to what previously observed for the Winnie model, 5 week-old Winnie-APC^{Min} mice were characterized by reduced body weight and colon length when compared to WT and APC^{Min} used as control (Figure

8C-E). These data were emphasized when the colon length was related to the mice weight (Figure 8F).

4.02: Winnie-APC^{Min} mice develop dysplastic lesions.

Histological analysis of 5-week old Winnie-APC^{Min} mice demonstrated the presence of dysplastic aberrant crypt foci (ACFs) along the all the colon length with a gradually increase in incidence and multiplicity moving from the proximal to the distal colon tract (Figure 9A-C). As expected, dysplastic ACFs are absent in the age-matched parental strains, excepted for APC^{Min} mice that showed a lower incidence and multiplicity for the neoplastic lesions as compared to the Winnie-APC^{Min} mice (30% Vs 78% of incidence and a multiplicity of 0.3 ± 0.15 Vs 2.2 ± 0.62 , respectively). The dysplastic ACFs were grouped according to the classification of neoplastic pre-invasive intraepithelial lesions of the colonic mucosa. No lesions showed the proliferative compartment located above the muscularis mucosa at the basal level. The aberrant crypts were classified by two grade of dysplasia: low (mild and moderate) and high (severe). The most recurring dysplasia grade was the moderate one, with low cigar-shaped-like nuclear crowding up to the lumen of the crypt. Atypical mitosis was observed rarely. Dysplastic ACFs were carefully characterized for incidence and multiplicity based on the number of crypts and the grading into four groups: unicroptic lesions; microadenoma $>1 \leq 5$ Low Grade (LG); microadenoma >5 Low

Grade (LG) and microadenoma >5 High Grade (HG). All of them showed a tubular pattern.

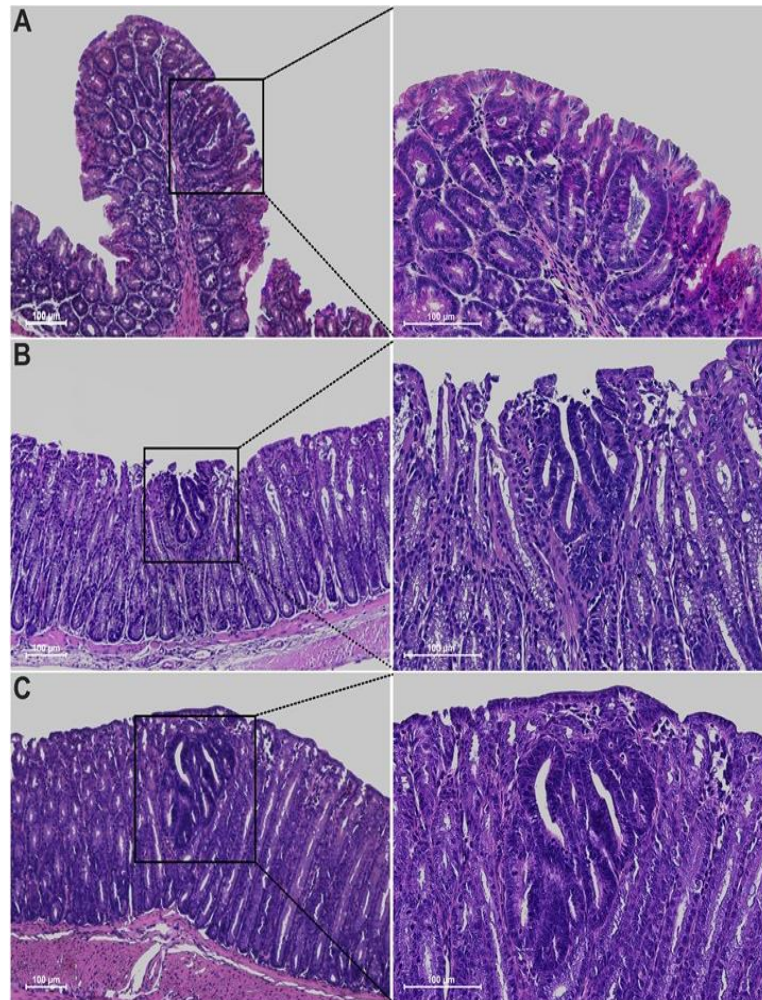


Figure 9: Histological characterization of the Winnie-APCMin murine model. Hematoxylin and eosin staining on 3 μ m colon sections from proximal (A), medial (B) and distal (C) tract of 5 week-old Winnie-APCMin mice. Images were captured at 10X (left) and 20X magnifications (right) [De Santis et al. Submitted Feb. 2019].

Winnie-APCMin mice also showed a low incidence and multiplicity of non dysplastic ACFs specifically in the medial tract of the colon. A similar incidence and multiplicity for this type of lesions is observed in the proximal tract of age-matched APCMin mice. Moreover, Periodic

Acid Schiff (PAS) staining reveals an overall decrease in mucin expression in the distal colon of Winnie and Winnie-APC^{Min} mice as compared with WT and APC^{Min} mice (Figure 10). Specifically, mucins

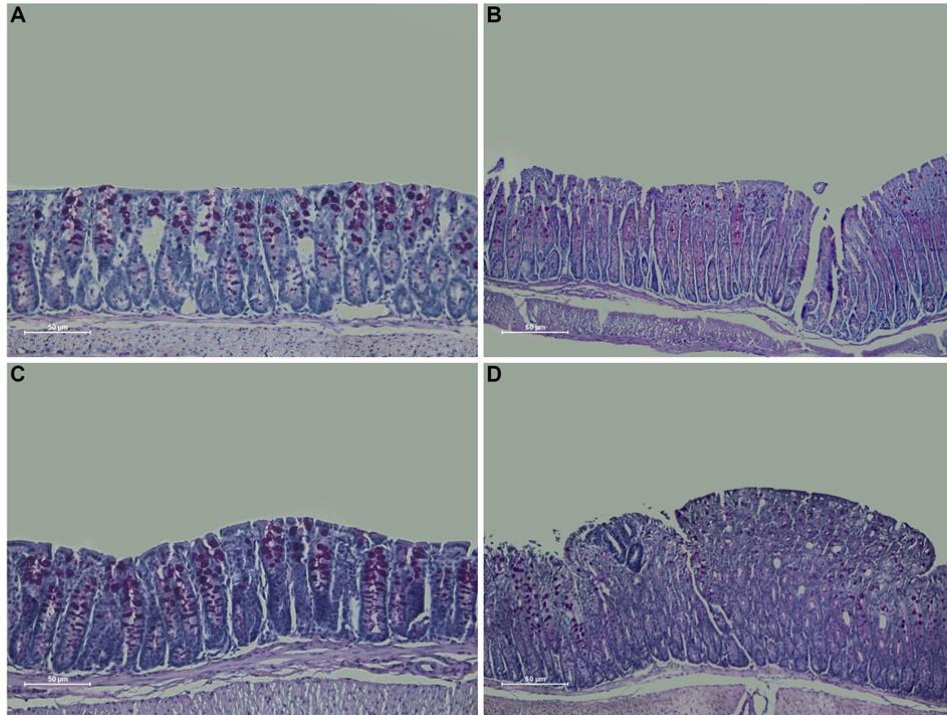


Figure 10: Mucins expression in presence of dysplasia. Periodic Acid Schiff (PAS) staining to highlight mucin expression in the distal colon of WT (A), Winnie (B), APC^{Min} (C) and Winnie-APC^{Min} (D) mice [De Santis et al. Submitted Feb. 2019].

4.03: 5 week-old Winnie-APC^{Min} mice gene expression.

The expression profile was evaluated from 5 week-old mice after obtaining mice genotype. RNA from the distal colon of 5 week-old Winnie-APC^{Min} mice and all the parental strains was analysed by qPCR comparing the expression of 89 selected genes for CRC. Compared to WT, the number of genes regulated at 5 week by Winnie and Winnie-APC^{Min} mice was higher than the ones modulated by APC^{Min} mice (26

and 28 Vs 8, respectively) (Figure 11A). Among the 27 genes resulting from the Winnie-APC^{Min} Vs WT analysis, more than a half was in common with Winnie (10 up and 6 down) and only one gene was shared with the molecular pattern of APC^{Min} mice (down). On the contrary, when comparing Winnie and APC^{Min} mice to WT, they only shared two genes that had a contra-regulation (Figure 11A).

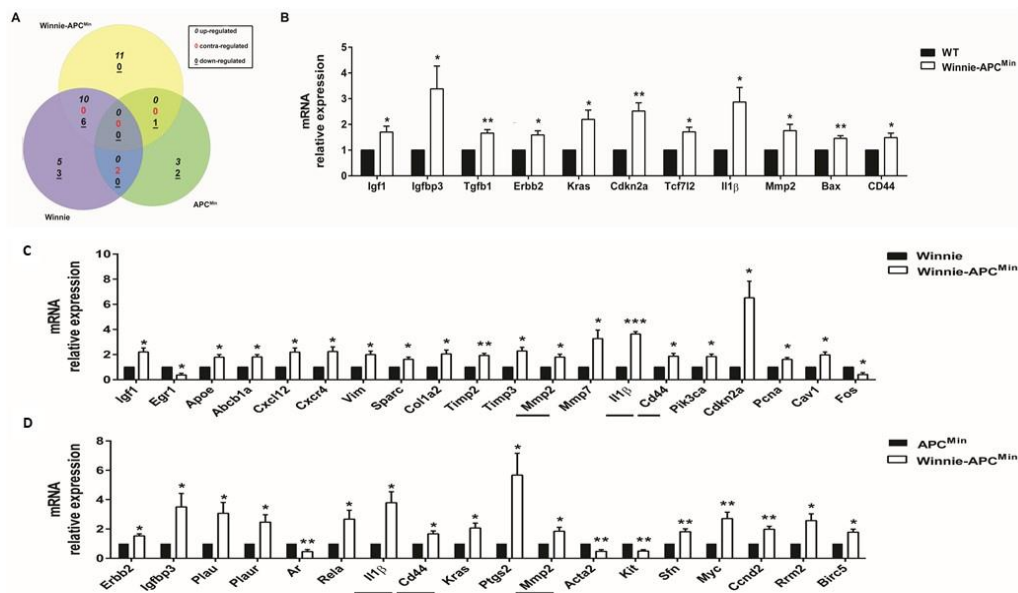


Figure 11: Molecular characterization of 5-week-old Winnie-APC^{Min} distal colon. (A) Venn diagram reported qPCR data obtained comparing Winnie-APC^{Min}, Winnie and APC^{Min} relative to WT mice. (B) Histogram indicates relative expression of 10 specifically up-regulated genes in Winnie-APC^{Min} (white bars) versus WT mice (black bars) (C) Winnie-APC^{Min} (white bars) versus Winnie mice (black bars) (D) Winnie-APC^{Min} (white bars) versus APC^{Min} mice (black bars) (n=3 animals/group). Histograms represent the mean of $2^{-\Delta\Delta Ct} \pm SEM$. *p<0.05, **p<0.01. [De Santis et al. Submitted Feb. 2019].

10 genes specifically up-regulated in Winnie-APC^{Min} Vs WT mice confirmed the modulation of genes known to be involved in CRC progression both in mice and humans (Figure 11B). We then compared

Winnie-APC^{Min} with Winnie and APC^{Min} mice; the number of modulated genes is approximately the same (Figure 11 C, D). Only 3 genes (IL-1 β , CD44 and Mmp2) were similarly upregulated in Winnie-APC^{Min} mice regardless if compared with Winnie or APC^{Min} (Figure 11).

4.04: Metagenomic analysis in 4 week-old Winnie-APC^{Min} mice.

Stools were collected from 4-week old mice when separated from the breeding cage. Metagenomic analysis was performed comparing bacterial relative abundance of Winnie-APC^{Min} mice with all the parental strains. The phylum profile reveals that Winnie-APC^{Min} are characterized by a microbiota intermediate between Winnie and APC^{Min} (Figure 12 A). The only exception is represented by the increased ratio between the abundance of Bacteroidetes and Prevotella in Winnie-APC^{Min} (Figure 12 B). This observation is important as Prevotella has been reported to be increased in colorectal cancer [33].

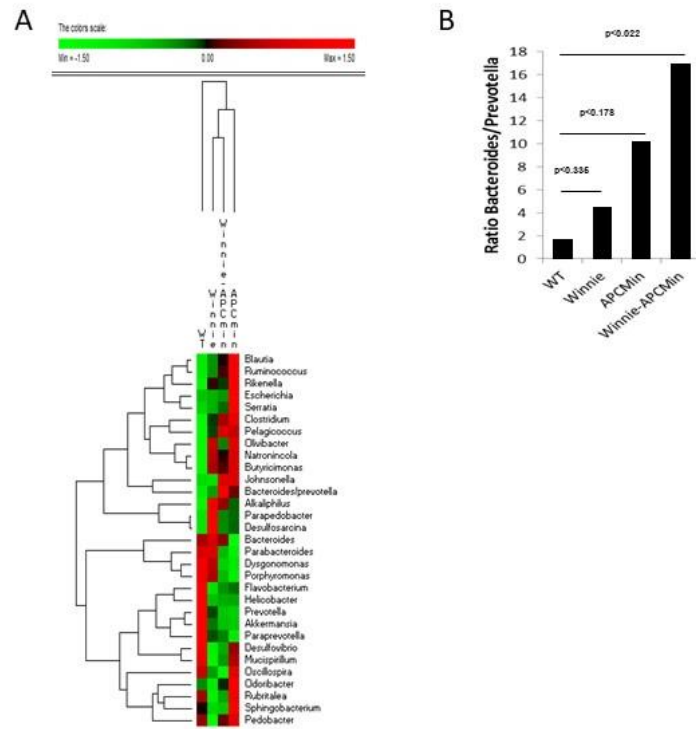


Figure 12: The phylum profile in the stools of Winnie-APCMin. Average relative abundance of the different phyla in 4-week old Winnie-APC^{Min} mice and all the parental strains. (n=4 animals/group) [De Santis et al. Submitted Feb. 2019].

Nutritional strategies to reduce inflammation

In parallel with the development of the Winnie-APC^{Min} mice we explored the possibility to prevent intestinal inflammation using nutritional derived bioactive compounds. Together with numerous other research group, we already reported the anti-inflammatory potential of numerous natural bio-active compounds as potential candidate for prevention and treatment of the intestinal inflammatory response. [21] The possibility to suppress the inflammatory response may also reduce the risk to develop CRC even more if used in combination with classical therapies. Plant polyphenols represent one of the largest and most ubiquitous groups of secondary metabolites that are an integral part of the human diet [34]. These compounds are characterized by the presence of one or more phenol rings and two or more hydroxyl groups linked directly to the aromatic rings [35] and have been associated with anti-oxidant, anti-microbial, anti-proliferative and anti-inflammatory properties [36, 37]. Despite evidence for the biological effects of these phytonutrients being reported, knowledge of the underlying molecular mechanisms activated upon polyphenols treatment remain poorly understood [38, 39].

4.05: Quercetin induces Slpi expression in LPS-activated BMDCs

In 2015, we published the results of a whole-genome microarray analysis performed on mRNA extracted from Quercetin and Piperine Reconstituted Oil Bodies (ROBs-QP) treated bone marrow derived

dendritic cells (BMDCs) at 6 hours post LPS exposure identified a number of genes that were significantly modified by polyphenols exposure as previously described [29]. As expected, most of the transcripts differentially expressed by polyphenol exposure were those of pro-inflammatory genes, which were significantly down-regulated consistent with known anti-inflammatory activity of the polyphenols. We identified secretory leukocyte protease inhibitor (Slpi) among the transcripts differently up-regulated in polyphenol exposed BMDCs following LPS stimulation (2.7-fold, $P < 0.01$; Figure 13). The microarray data was confirmed by qPCR where Slpi expression was significantly up-regulated in the ROB-s-QP treated BMDCs reaching a 26-fold ($P < 0.01$) increase at 24h post LPS activation compared to a 4-fold increase in vehicle treated BMDCs. Significantly, Slpi expression was increased in ROB-s-QP treated BMDCs even before LPS activation (7-fold induction) (Figure 13B) [40].

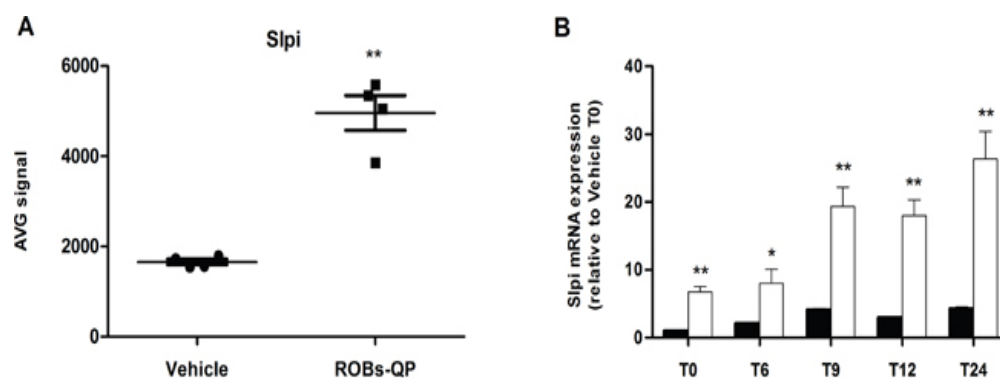


Figure 13: Quercetin induces Slpi expression in LPS-activated BMDCs. **A.** Slpi expression from the microarray data of BMDCs exposed to vehicle or ROB-s-QP at day 5 and 7 and treated with 1 $\mu\text{g}/\text{mL}$ of LPS for 6 hours ($n=4$, $**P < 0.01$). **B.** Time course mRNA expression of Slpi mRNA measured by qPCR of BMDCs exposed to vehicle (black bars) or ROB-s-QP (white bars) at day 5 and 7 and treated with 1 $\mu\text{g}/\text{mL}$ of LPS. Fold change are expressed relative to vehicle at time 0. mRNA was extracted at indicated time points and bars represent the mean \pm SEM of 3 independent experiments. ($*P < 0.05$, $**P < 0.01$) [40].

Similar Slpi expression profiles were obtained using 25 μ M of synthetic quercetin (data not shown). For this reason, we chose to study the effect of a single polyphenol administration and used synthetic quercetin for the remainder of the study.

4.06: Quercetin reduces TNF α secretion by up-regulating Slpi

As already known, BMDCs isolated from WT mice and treated with quercetin showed a significant reduction in secretion of TNF α upon activation with LPS compared to non-treated BMDCs (50% suppression, $P < 0.01$). To demonstrate the crucial importance of Slpi we treated BMDCs from Slpi-KO mice in the same way and observed that DCs failed to reduce TNF α secretion (Figure 14A). To further elucidate whether the observed difference in TNF α secretion in quercetin treated BMDCs from WT and Slpi-KO mice was indeed Slpi dependent we used siRNA to knockdown Slpi in WT BMDCs and assessed the TNF α secretion profile. siRNA knockdown of Slpi in BMDCs from WT mice (at day 4 of culture) also demonstrated a failure to reduce TNF α secretion after quercetin treatment and LPS activation (Figure 14B). In contrast, BMDCs from WT mice that had Slpi expression knocked-down after quercetin treatment (at day 6 of culture) suppressed TNF α secretion after exposure to LPS similar to mock siRNA treated BMDCs (Figure 14C) [40].

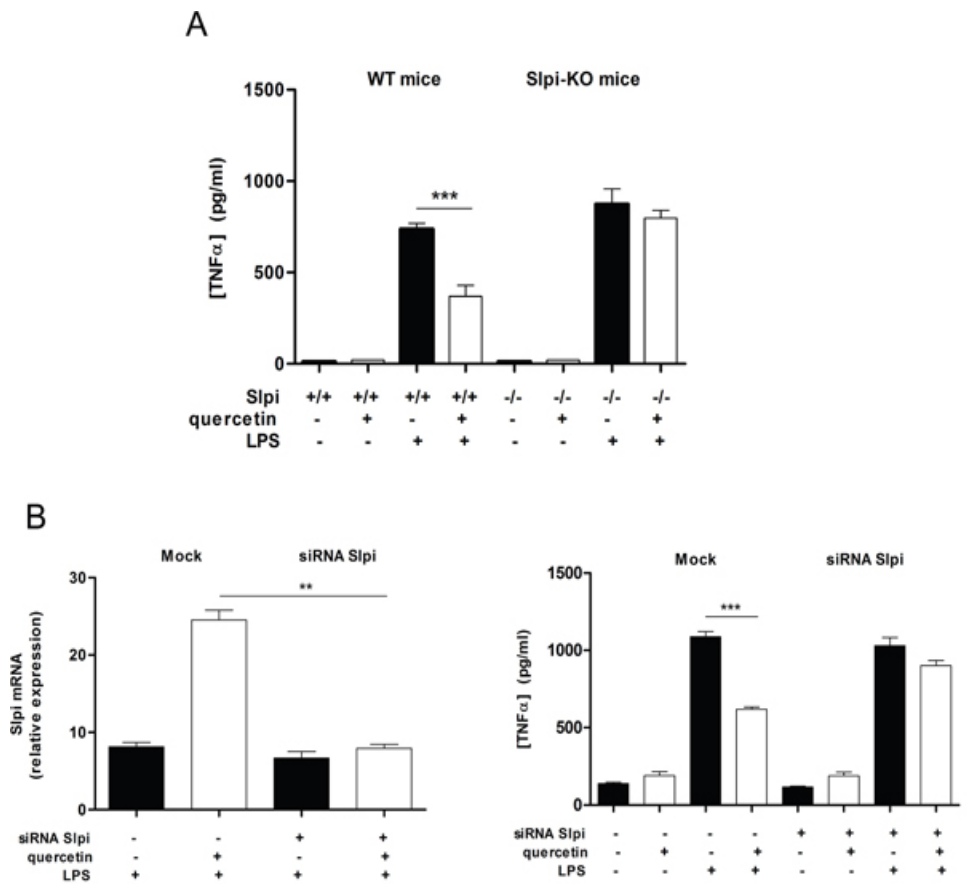


Figure 14: Quercetin reduces TNF α secretion by up-regulating Spli. **A.** BMDCs were cultured from WT and Spli-KO mice and treated with quercetin at day 5 and 7. BMDCs cultures were exposed to 1 μ g/mL of LPS and the secretion of TNF α was determined by ELISA after 24 hours. Bars represent mean cytokine concentration \pm SEM (n=4) for BMDCs from WT or Spli-KO mice treated with and without quercetin (black and white bars, respectively), ***P<0.001). **B.** BMDCs were transfected with siRNA for Spli and Lipofectamine[®] 3000 reagent (mock) at day 4, before the administration of quercetin. qPCR for Spli demonstrated a good efficiency for siRNA transfection (left). Bars represent a mean fold change \pm SEM (n=3) between LPS stimulated BMDCs +/- quercetin relative to LPS unstimulated cells +/- quercetin, respectively. **P<0.01. The secretion of TNF α was determined 24 hours after LPS stimulation by ELISA (right). Bars represent mean cytokine concentration \pm SEM (n=3) for DCs treated with and without quercetin (black and white bars, respectively). ***P<0.001. **C.** BMDCs were treated with quercetin on day 5 and transfected with siRNA for Spli at day 6 followed by quercetin administration at day 7 and a subsequent exposure to LPS on day 8. A good reduction in Spli expression was observed by qPCR analysis (left). Bars represent a mean fold change \pm SEM (n=3) between LPS stimulated BMDCs +/- quercetin relative to LPS unstimulated cells +/- quercetin, respectively. **P<0.01. The secretion of TNF α was determined 24 hours after LPS stimulation by ELISA (right). Bars represent mean cytokine concentration \pm SEM (n=3) for DCs treated with and without quercetin (black and white bars, respectively). *P<0.05 [40].

4.07: Quercetin effects are lost enriching the culture media with iron

Once realized that we unveiled a pivotal molecular pathway involved in quercetin inflammatory-suppressor ability, we focused our attention to the mechanism that triggers the inflammatory suppression. Several polyphenols exhibit numerous properties including phytochelation; the ability to complex metal ions, including highly reactive iron. Dendritic cell inflammatory response is also associated with modulation of several iron metabolism related genes. Under inflammatory conditions, macrophages, but also monocytes and dendritic cells (DCs), retain iron through ferritin, an intracellular protein that can bind up to 400 atoms of iron. At the same time, iron export is inhibited due to the cascade of events that is triggered by inflammation-mediated increased levels of hepcidin. Hepcidin binds to the iron-export protein ferroportin and consequently induces its internalization and degradation. The overall result is a decreased level of circulating iron and increased load of cytoplasmic iron in macrophages [41].

From the aforementioned microarray, we extracted data demonstrating that quercetin exposure induced Ferroportin 1 Fpn1 expression (data not shown), thus we expected reduced intracellular iron concentration of iron in quercetin-treated DCs. With the intent to visualize iron intracellular content, DCs were plated into glass bottom cell Culture dishes, at day 7, 1 μ M of iron was added in the culture media, with quercetin (25 μ M) or same volume of vehicle (1 μ l DMSO/1ml media). LPS was then added 24 hours later and 6 hours later, cells were

stained with the Iron Stain Kit. Figure 15A shows strong cytoplasmic blue color into LPS treated cells, while quercetin presence severely reduced cells positivity. We quantified the blue signal intensity in 30 different images obtained from 3 separated experiments (Figure 15B). We then compared Hmox1 protein expression in DCs lysate 24h after LPS administration. Figure 15C shows the immunoblot of vehicle or quercetin exposed DCs in presence or absence of LPS. Vehicle and quercetin treated DCs expressed similar level of Hmox1, while LPS administration significantly reduced it. Importantly, when LPS was administered to quercetin-exposed DCs, Hmox1 signal was higher than control. To investigate the axis between iron chelation and quercetin, we additioned different concentration of iron in the DCs culture media. Figure 15D shows the LPS induced secretion of IL-6 and IL-12p70 by DCs treated with quercetin or vehicle. The left side of the figure 15D shows the quercetin induced reduction of LPS-induced IL-6 and IL-12p70 secretion. Quercetin efficiency is gradually lost in presence of increasing doses of iron. Indeed, administration of 2 μ M of iron was able to revert quercetin mediated IL-6 and IL-12p70 suppression [42].

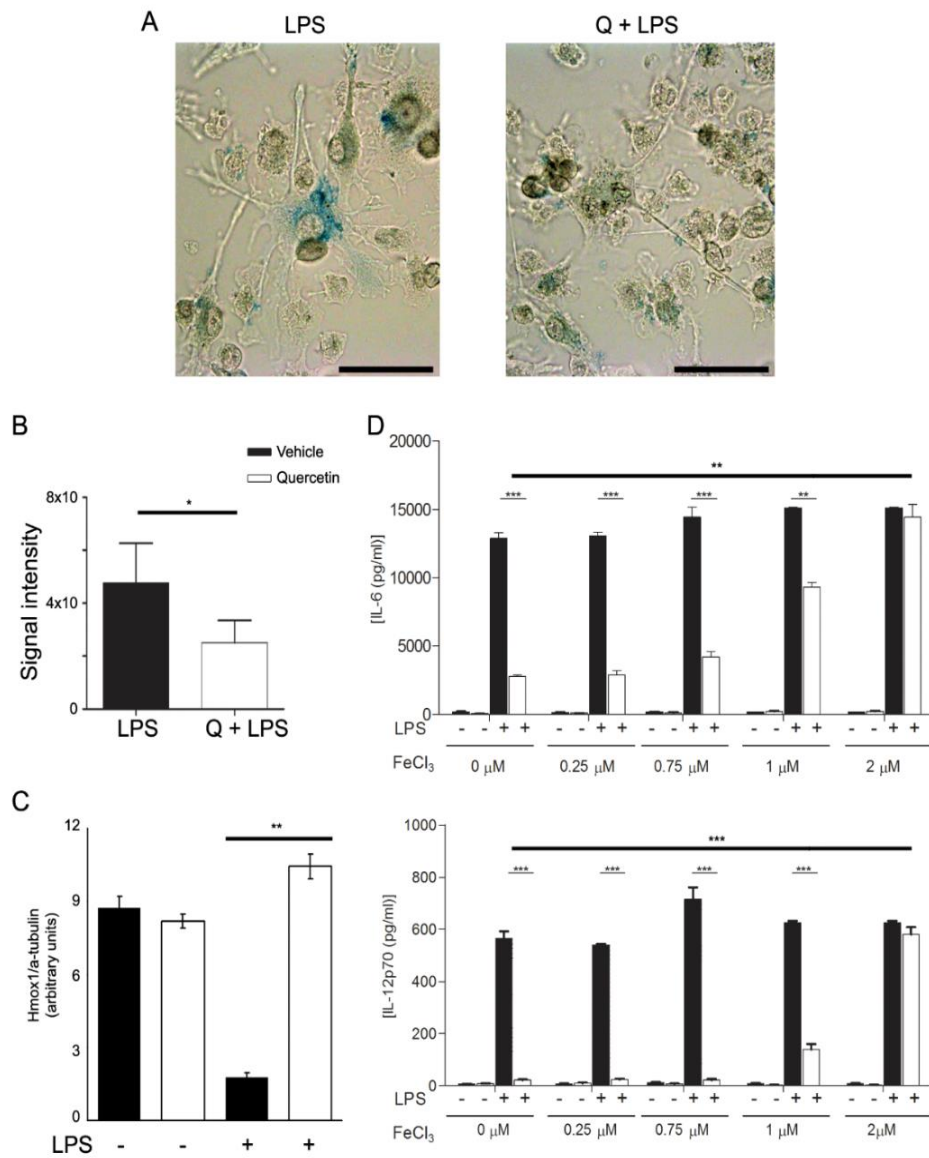


Figure 15: Quercetin effects are lost in presence of high doses of iron in the culture media. Histological staining for the determination of ferrous pigment in BMDCs, fixed paraformaldehyde 1% (A). LPS treated dendritic cells (right panel) and quercetin-exposed dendritic cells (left panel) cultured in FeCl₃ (1 μM) enriched media. Blue signal intensity was quantified in 30 different images obtained from 3 separated experiments. Scale bar is 50 μm. The histogram (B) represents the mean blue signal intensity for the iron staining ± SEM. C) Western blot analysis of BMDCs lysate 24h post LPS administration. The histogram represents the ratio between Hmox1 and tubulin bar quantification obtained from 3 different experiments. Panel D shows the LPS-induced secretion of IL-6 and IL-12p70. Quercetin (white bars) or vehicle (black bars) DCs were treated with FeCl₃ and LPS at the indicated doses, IL-6 and IL-12p70 were determined by ELISA. Bars represent mean cytokine concentration ± SEM of 3 independent experiments. *P<0.05; **P<0.01; ***P<0.001 [42].

4.08: Gut Microbiota Respond to the Iron Starvation

It has long been known that iron availability is crucial for bacterial growth, and iron deprivation is an efficient strategy to limit bacterial growth. Recently, an increased risk of bacterial infections has been observed following the administration of non-physiological amounts of iron and, in particular, an increased virulence of *Escherichia*, *Klebsiella*, *Listeria*, *Neisseria*, *Pasteurella*, *Shigella*, *Salmonella*, *Vibrio*, and *Yersinia* [43]. When studied using murine models of colitis, the increased oxidative stress was identified as the major cause of disease exacerbation following oral iron administration, but several other mechanisms may be important, including endoplasmic reticulum stress, a microbial community shift and immune cells activation. Furthermore, *in vitro* results obtained using the intestinal fermentation model described by Cinquin et al. [44] demonstrated a direct link between iron restricted growth condition and the growth advantage obtained by *Enterobacteriaceae* and *Lactobacilli* [45]. Nonetheless, these *in vitro* results were in contrast with Dostal et al. who observed marginal changes in gut microbiota composition in rats under low luminal Fe concentrations [46].

Thanks to the collaboration with Prof. Cathie Martin in Norwich (UK) we had the opportunity to use a new transgenic tomato line called *Bronze*, to enrich mice chow with natural polyphenols [47]. We investigated any impact of the different tomato-supplemented diets on probiotic groups, whose growth is relevant to intestinal health (Figure

16). We developed different custom diets supplemented with 1% lyophilized fruit from the different tomato lines (wild type, Indigo, ResTom, and Bronze) and administered them to age- and sex-matched C57Bl/6 mice, for 2 weeks. In particular, mice fed with diets enriched with Bronze and ResTom tomato fruit were characterized by a significant increase in the phylum Bacteroidetes and a decrease in Firmicutes, resulting in a significant increase ($P < 0.05$) in the ratio of Bacteroidetes to Firmicutes which doubled from 0.86 in mice fed the standard diet to 1.74–1.79 in mice fed diets enriched with 1% ResTom and 1% Bronze tomato fruit, respectively (Figure 16C). These data suggested that dietary stilbenoids promoted growth of Bacteroidetes over Firmicutes in mice.

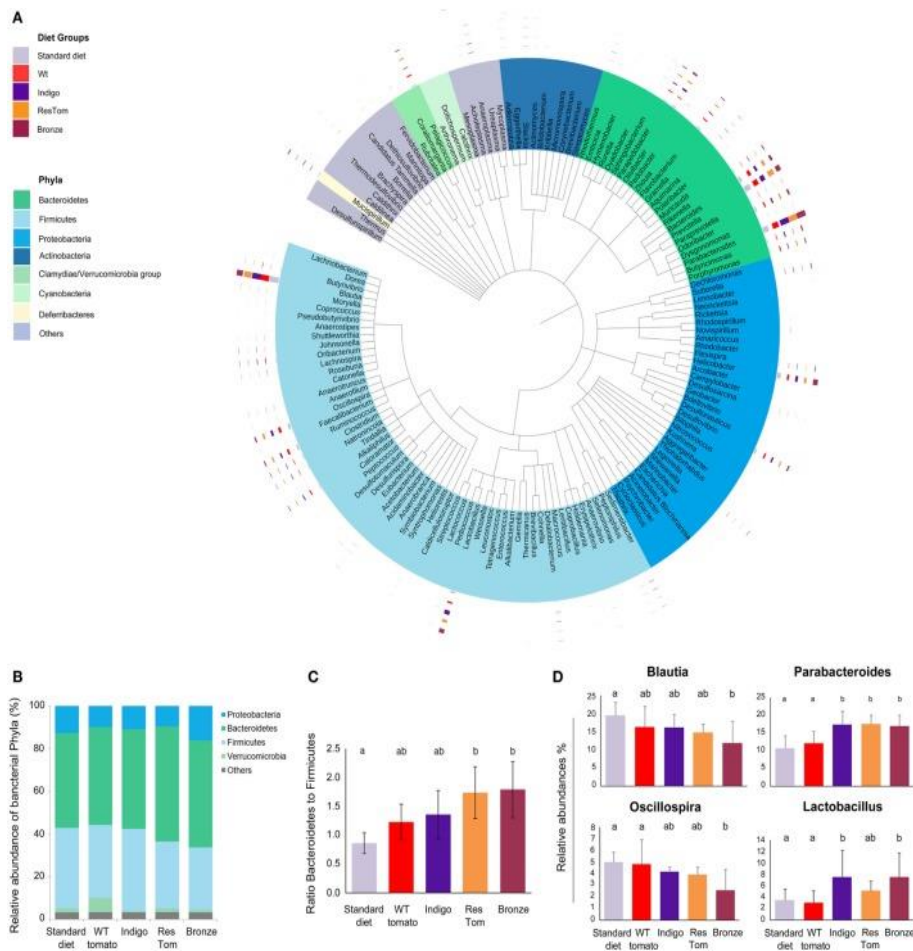


Figure 16: Composition of the intestinal microbiota of mice fed diets enriched with different tomato fruit. Sex-matched mice ($n = 5$) were divided into five groups, based on the diet (standard diet and diets enriched with 1% of wild-type, Indigo, ResTom, and Bronze lyophilized tomato fruit). After 2 weeks diet, fecal samples were collected for the microbiota meta-analysis. (A) Circular representation of the phylogenetic tree showing the major 150 genera of the intestinal microbiota. The inner bands indicate the genera colored by phylum. The outer circles show multibar charts indicating the relative abundances of genera in different diet groups. (B) Relative abundances of the phyla found in the microbiome of mice in different diet groups. (C) Bacteroidetes/Firmicutes ratio in the microbiome of mice fed with different diets. (D) Relative abundances of the genera of the microbiome showing significant differences among diet groups. The letters above the histograms in panels (C) and (D) indicate the significant differences between two different diet groups assessed by Duncan's multiple-range test [47].

4.09: Effects of nutritional intervention in Winnie mice

We demonstrated that the administration of a nutritional regime enriched with 1% of Bronze tomato fruit was able to promote a change in the composition of the microbiota in healthy mice and partially suppress the host inflammatory response to reduce/delay the appearance of intestinal damage induced by DSS administration [47].

In contrast to the previous experimental setup, we built on our published findings and used the murine model of spontaneous UC, Winnie, to investigate the therapeutic rather than the preventive potential of the Bronze-enriched diet. Our aim was to determine the therapeutic potential of a dietary intervention based on the Bronze-enriched diet in adult Winnie mice.

We explored the effects of nutritional intervention in a model of spontaneous progressive ulcerative colitis. WT and Winnie mice were fed for 2 weeks with 1% control (Control) or bronze (Bronze) tomato-enriched diets. Figure 16A shows the experimental setup. Administration of the enriched diets did not alter the weight of WT and Winnie mice (Figure 16B) nor their colon weight and length (Figure 16C, D, respectively). Morphological analysis of the explanted colon did not reveal differences between Control and Bronze treated mice (data not shown) [48].

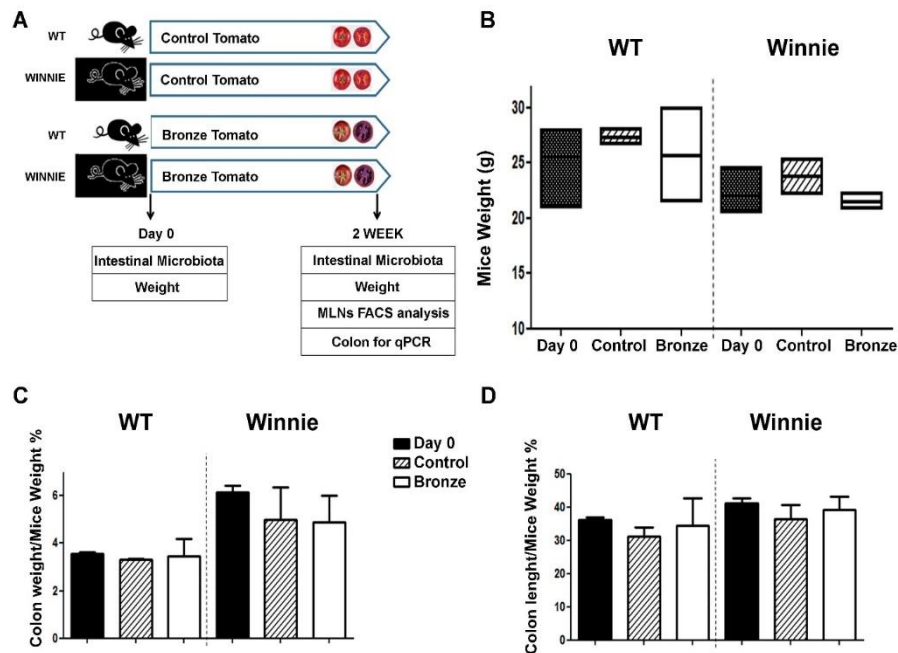


Figure 17. Experimental design and macroscopic characterization of the experimental groups. (A) Sex-matched mice were divided into four groups based on their genotype (Wild Type or Winnie) and their diet (enriched with Control or Bronze lyophilized tomato fruit). Mouse weight was recorded at the beginning of diet administration (Day 0) and at the end of the trial (2 Weeks). Fecal samples were collected for microbial meta-analyses at both time points (Day 0 and Week 2). Tissues were explanted and analyzed at the end of the treatments as indicated. Analysis of mice from different groups included: mouse weight (B), colon weight/mouse weight (C) and colon length/mouse weight (D). Black bars show the values at Day 0, striped bars show the Control- and white bars the Bronze-enriched diet. Statistical evaluation was performed using unpaired two-tailed Student's t-tests [48].

4.10: IL-17A Reduction in CD4+ Mesenteric Lymph Node (MLN) T Cells Treated with a Bronze Tomato Diet

Following two weeks of tomato-enriched diets, we isolated and analyzed the intracellular cytokine production of the MLNs CD4+ T cells. The Bronze enriched diet resulted in a reduced percentage of CD25+Foxp3+ (Figure 18A) and increased percentage of TNF α + cells (Figure 18B) compared to the Control diet. Both changes were not

significantly different, but the trend was consistent independent of the genotype of the mice. A Bronze diet resulted in a significant reduction in the percentage of IL-17A CD4⁺ cells in WT mice and a similar trend in Winnie mice, while the percentage of IFN γ +CD4⁺ cells was unchanged (Figure 18C) both in WT and Winnie. Of note, the percentage of IFN γ +CD4⁻ cells was reduced by the Bronze diet, particularly in Winnie mice (Figure 18D) [48].

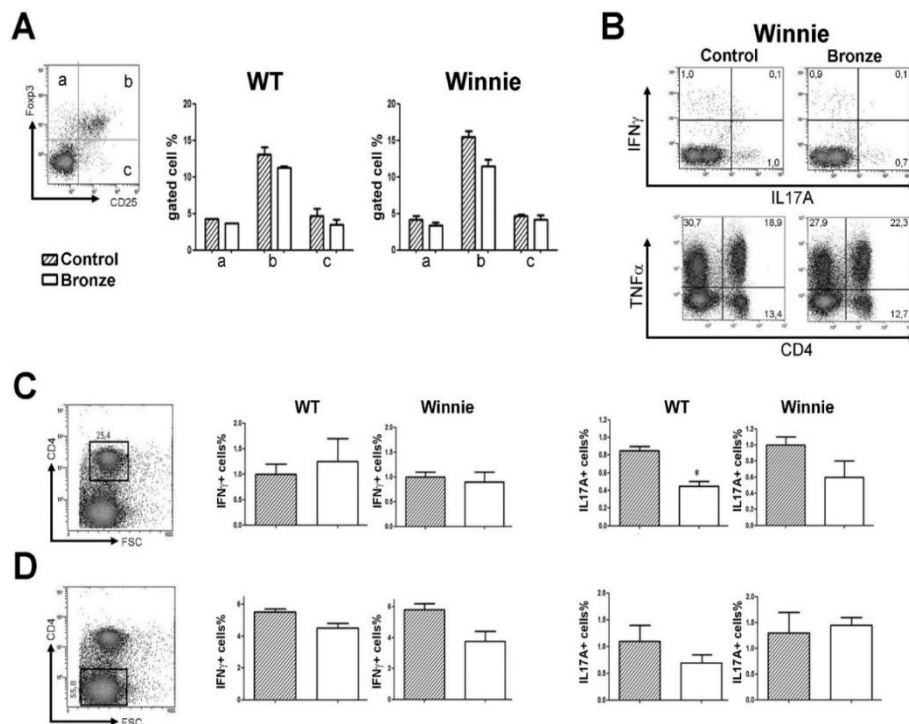


Figure 17. Mesenteric lymph node T cell cytokine staining. (A) Representative Treg staining of CD4⁺ cells. Histograms represent the percentages of Foxp3+CD25⁺ cells in the MLNs of mice fed with Control-enriched diet (striped bars) and Bronze-enriched diet (white bars). (B) Representative density plot analysis of intracellular staining of MLNs from Winnie mice. (C, D) Intracellular staining of IFN γ and IL-17A in the CD4⁺ (C) and CD4⁻ (D) MLN cells of WT and Winnie mice after 2 weeks of Control or Bronze-enriched diets. Statistical evaluation was performed using unpaired two-tailed Student's t-tests. * P < 0.05 [48].

4.11: Bronze Tomato Diet Molecular Signature

We previously demonstrated that the administration of a Bronze enriched diet was able to reduce the expression of inflammatory cytokines (Il-6, Tnf- α , Il-1 α , Il-1 β , Il-12) in the colon of WT mice [29] and that the expression level of Slpi was a reliable marker for the oral intake of quercetin [40, 49]. We next analyzed the expression levels of Tnf- α , Ifn γ , Il-10, Slpi and Hmox1 in the colon of WT and Winnie mice. While both a Bronze and Control enriched diet significantly increased Il-10 expression in WT mice (Figure 18A), only a Bronze diet induced a higher increase in Il-10 in Winnie mice. Tnf- α and Ifn γ colon expression was generally lower in mice fed with Control or Bronze diets in both the Winnie and WT mice (Figure 18B,C). A significant reduction in Ifn γ expression was observed in Winnie mice fed with a Bronze diet compared to Day 0, but not in Winnie mice fed with a Control diet. Slpi, a major checkpoint for the anti-inflammatory activity of quercetin [40, 48], was significantly induced by both the Control and the Bronze-enriched diets both in WT and Winnie mice (Figure 18D). Slpi induction was higher in Winnie compared to WT mice. Hmox1 expression was similar to that of Slpi, suggesting an anti-inflammatory pathway that is induced by the Bronze diet (Figure 18E).

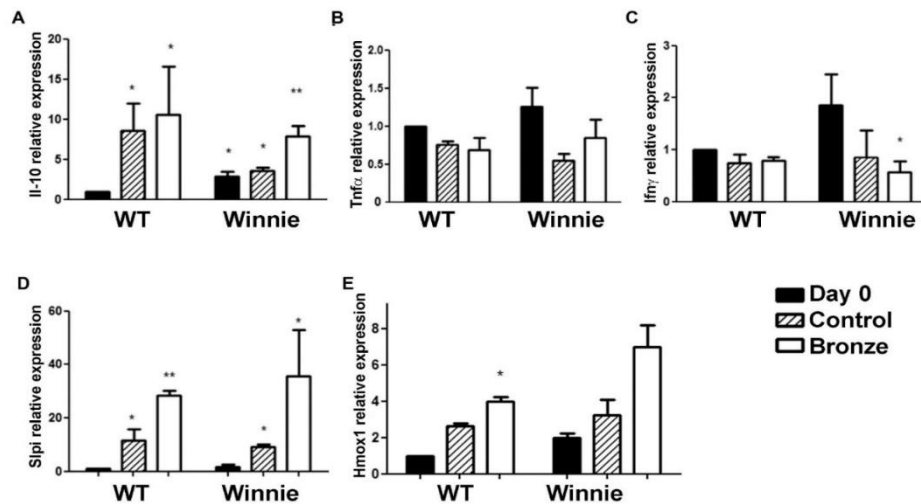


Figure 18. Two weeks of Bronze-enriched diet induced Sipi and Hmox1 expression in the medial colon of WT and Winnie mice. Histograms represent the average expression of IL-10, Tnf- α , Ifn γ , Sipi and Hmox1 (A–E respectively) measured by real time PCR in the medial colon of WT and Winnie mice after two weeks of Control- (striped bars) and Bronze-enriched diet (white bars). Black bars represent the gene expression at Day 0. All bars represent mean expression \pm SEM for each treatment. Control and Bronze dependent expression were compared to WT Day 0 for the statistical evaluation. Student's t-test was used to compare every measurement to the corresponding WT Day 0 and evaluate the significance of the data. ** P < 0.01, * P < 0.05 (Student's t-test). Grouped analyses were performed with the two-way ANOVA test, using Bonferroni as a post test ANOVA p Value: IL-10: p = 0.0348; TNF α : p = 0.0523 IFN γ : p = 0.6483 Sipi: p = 0.0058 HMOX: p = 0.0002 [48].

4.12: Dysbiotic Intestinal Microbiota Communities Changed Following Two Weeks on a Bronze Tomato Diet in Winnie Mice

Time zero for each mouse was collected both for WT and Winnie mice. At day 0 for the mice fed with Control tomato-enriched diet, the Shannon index of the Winnie mice was higher than the WT mice (2.413 and 2.180, respectively, P = 0.011). No statistically significant differences were found for the number OTUs and Chao index. To investigate the response of the microbiota to the host intake of different dietary regimes, fecal material was collected from mice following two weeks of Bronze or Control enriched chow. After two weeks of feeding Control tomato, the

WT mice increased their OTUs and their Shannon index compared to Day 0. Compared to the Control tomato diet, all WT and Winnie mice showed non-significant reductions in OTUs on the Bronze tomato diet. In our previous studies, the diversity and richness of the microbiota of mice did not show significant differences ($P > 0.05$) in response to different diets [47]. The 3 phylogeny-based β -diversity analyses did not show statistical separation between the composition the microbiome of fecal mouse samples after two weeks of Bronze or Control tomato diets. Samples were mainly clustered according to the genotype (WT or Winnie mice).

The evaluation of the 16S revealed a significant difference ($P < 0.05$) between 20-week old WT and Winnie mice. In particular, the relative abundance of Bacteroidetes and Firmicutes (41.97% and 39.26% in WT vs. 60.62% and 23.36% in Winnie mice), as well as the ratio between them (1.14 vs. 2.76 respectively, $P = 0.022$) confirmed differences already known for hosts characterized by ongoing intestinal inflammation [50,51]. Two weeks of dietary intervention changed the microbial content of both WT and Winnie mice. The differences in bacterial abundance monitored by 16S segregation, observed at time zero, were later lost as fecal material from WT and Winnie mice could not be clearly differentiated (Figure 19).

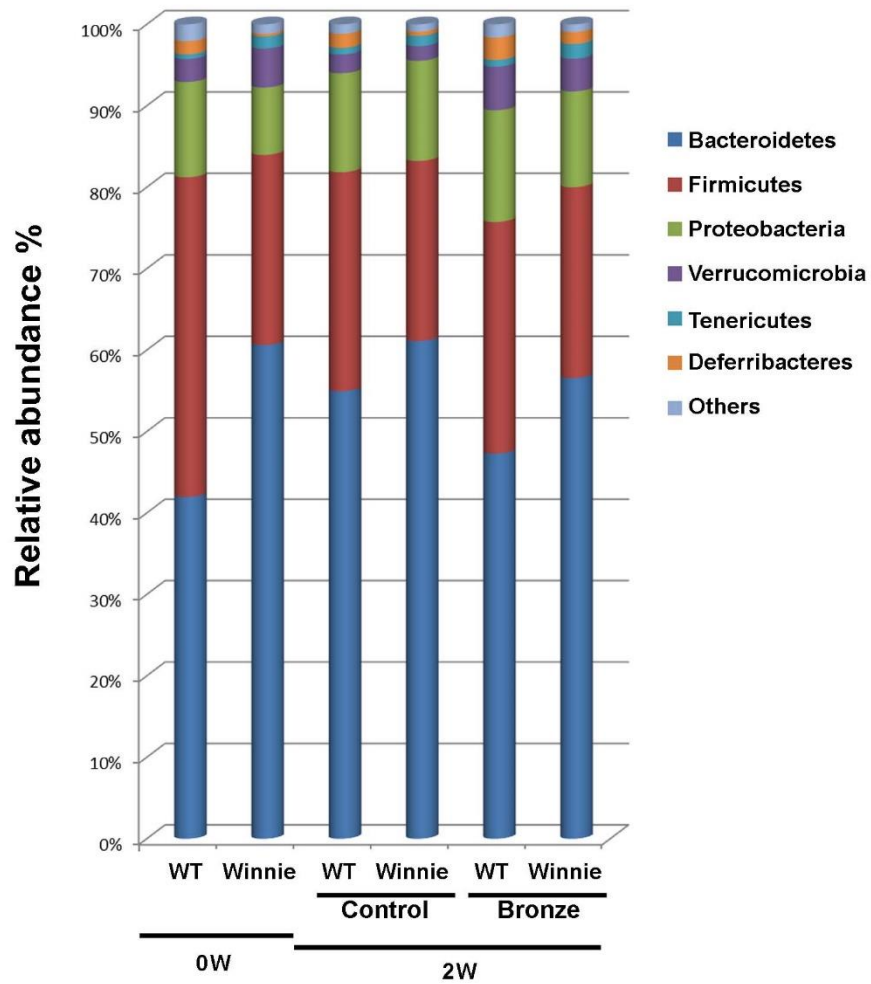


Figure 19. Total bacteria found in feces of WT and Winnie mice. Relative abundance (%) of total (16S rRNA) bacteria, found at the phylum level in the fecal samples of WT and Winnie mice at Day 0 (0W) and after two weeks (2W) on Bronze (Bronze) or Control tomato (Control) diets [48].

5. CONCLUSIONS

During these last three years of PhD we aimed to create a new murine model of spontaneous inflammatory-induced colorectal cancer a combining the genetic susceptibility of the APC^{Min} model and the chronic intestinal inflammation of the Winnie mice. Currently, there is a sharp distinction between CRC and colitis-associated cancer (CAC) as clinical evaluations reveal that CRC tumors do not arise in the context of preceding inflammation [33]. Using murine models of CAC a single injection of carcinogen azoxymethane (AOM) is sufficient to give rise to multiple colonic tumors, when if chronic colitis has been induced, while it takes multiple injection of carcinogen and longer time for tumors to form when inflammation is absent [52, 53].

Differently from CAC, the most commonly used model of CRC is APC^{Min} that is genetically predisposed to develop intestinal cancer. APC^{Min} mice are often treated with DSS to induce colonic inflammation resulting in faster CRC development.

Differently from the DSS induced colitis, Winnie are murine models of spontaneous, mild and progressive ulcerative colitis that require several months to show histological sign of disease. During these years, we characterized the disease progression in Winnie [54]. 5-week old mice show reduced body weight, watery diarrhea, but now rectal bleeding or prolapse. Importantly, histologically no distinctive sign of UC is present in the colon, but a specific molecular pathway characterized by upregulated inflammatory cytokine transcript is present [54].

In light of the mild inflammatory response observed in 5-week old Winnie, it was surprising to realize that the colon of age matched Winnie-APC^{Min} mice was rich of

dysplastic ACFs along the all the colon length with a gradually increase in incidence and multiplicity moving from the proximal to the distal colon tract (Figure 9A-C). This feature is extremely relevant as our model underlines the importance of chronic inflammation in genetically predisposed patients, even if the inflammation is considered mild. For these patients, prevention may represent the only effective strategy to improve/prolong disease free periods. The Winnie-APC^{Min} molecular pathway underlines the unique molecular feature resulting from the combination of genetic predisposition and chronic inflammation. This still preliminary observation has been used to submit an experimental protocol aiming to prevent the upregulation of some of the Winnie-APC^{Min} specific genes using nutritional strategies that suppress the intestinal inflammation and/or prevent dysbiosis. Indeed, nutritional based strategies to suppress or mitigate intestinal inflammation has been one of the most important research topic of our group [21, 29, 30, 40, 48, 49]. In particular, during the the first decade of scientific career, the candidate contributed to understand the importance of intestinal resident DCs for the intestinal homeostasis and the complex dynamic of DCs recruitment and polarization in the intestinal lamina propria [55-60]. For this reason we used BMDCs as a paradigm of cells potentially affected by polyphenol exposure.

Dendritic cells respond to quercetin exposure producing secretory leukocyte protease inhibitor (SLPI). SLPI is an antimicrobial protein that is also involved in tissue repair and possess the ability to block NFkB nuclear translocation with the ultimate result to suppress inflammation [61]. Using Slpi-KO DCs we demonstrated that Slpi induction was a necessary step following quercetin administration to suppress inflammatory cytokine secretion, nonetheless the mechanism of action that triggers Slpi production was still not clear.

Using an easy dose response experiment, we demonstrated that the administration of inorganic iron was able to block quercetin in a dose dependent manner. As quercetin is a strong iron chelating agent [62, 63] we proposed that quercetin-iron chelation may result in DCs cytoplasmic loss of iron reservoir and consequent switch to an inflammatory-impaired phenotype [64, 65]. At the same time, nutritional intake of quercetin may contribute to sequester iron from the intestinal lumen, suppressing bacterial growth. This aspect was partially explored using polyphenol enriched diet administered to WT or Winnie mice. Dysbiosis is partially recovered after two weeks of 1% enriched diet. Currently ongoing experiments will demonstrate if enriched diet may be used as prevention strategies to suppress inflammation and prevent intestinal dysbiosis, particularly in the context of CRC genetically predisposed individuals.

The Winnie-APC^{Min} model will be crucial to evaluate the efficiency of the polyphenol-enriched nutritional strategies and, potentially, many different pharmaceutical approaches.

6. REFERENCES

1. Saldova R. Cause of cancer and chronic inflammatory diseases and the implications for treatment. *Discov Med.* 2016 Sep;22(120):105-119. Review. PubMed PMID: 27755966.
2. Kim ER, Chang DK. Colorectal cancer in inflammatory bowel disease: the risk, pathogenesis, prevention and diagnosis. *World J Gastroenterol.* 2014 Aug 7;20(29):9872-81. doi: 10.3748/wjg.v20.i29.9872. Review. PubMed PMID: 25110418; PubMed Central PMCID: PMC4123369.
3. Colotta F, Allavena P, Sica A, Garlanda C, Mantovani A. Cancer-related inflammation, the seventh hallmark of cancer: links to genetic instability. *Carcinogenesis.* 2009 Jul;30(7):1073-81. doi: 10.1093/carcin/bgp127. Epub 2009 May 25. Review. PubMed PMID: 19468060.
4. Sharan R, Schoen RE. Cancer in inflammatory bowel disease. An evidence-based analysis and guide for physicians and patients. *Gastroenterol Clin North Am.* 2002 Mar;31(1):237-54. Review. PubMed PMID: 12122735.
5. Al Bakir I, Curtius K, Graham TA. From Colitis to Cancer: An Evolutionary Trajectory That Merges Maths and Biology. *Front Immunol.* 2018 Oct 16;9:2368. doi: 10.3389/fimmu.2018.02368. eCollection 2018. Review. PubMed PMID: 30386335; PubMed Central PMCID: PMC6198656.
6. Bonovas S, Minozzi S, Lytras T, González-Lorenzo M, Pecoraro V, Colombo S, Polloni I, Moja L, Cinquini M, Marino V, Goletti D, Matucci A, Tocci G, Milano GM, Scarpa R, Cantini F. Risk of malignancies using anti-TNF agents in rheumatoid arthritis, psoriatic arthritis, and ankylosing spondylitis: a systematic review and meta-analysis. *Expert Opin Drug Saf.* 2016 Dec;15(sup1):35-54. Review. PubMed PMID: 27924644.
7. Dinarello CA. Differences between anti-tumor necrosis factor-alpha monoclonal antibodies and soluble TNF receptors in host defense impairment. *J Rheumatol Suppl.* 2005 Mar;74:40-7. Review. PubMed PMID: 15742464.
8. Corridoni D, Arseneau KO, Cominelli F. Inflammatory bowel disease. *Immunol Lett.* 2014 Oct;161(2):231-5. doi: 10.1016/j.imlet.2014.04.004. Epub 2014 Jun 2. Review. PubMed PMID: 24938525; PubMed Central PMCID: PMC4401421.
9. Podolsky DK. Inflammatory bowel disease. *N Engl J Med.* 2002 Aug 8;347(6):417-29. Review. PubMed PMID: 12167685.
10. Braegger CP, Nicholls S, Murch SH, Stephens S, MacDonald TT. Tumour necrosis factor alpha in stool as a marker of intestinal inflammation. *Lancet.* 1992 Jan 11;339(8785):89-91. PubMed PMID: 1345871.
11. Khanna PV, Shih DQ, Haritunians T, McGovern DP, Targan S. Use of animal models in elucidating disease pathogenesis in IBD. *Semin Immunopathol.* 2014 Sep;36(5):541-51. doi: 10.1007/s00281-014-0444-6. Epub 2014 Sep 12. Review. PubMed PMID: 25212688; PubMed Central PMCID: PMC4205729.
12. Moser AR, Luongo C, Gould KA, McNeley MK, Shoemaker AR, Dove WF. ApcMin: a mouse model for intestinal and mammary tumorigenesis. *Eur J Cancer.* 1995 Jul-Aug;31A(7-8):1061-4. Review. PubMed PMID: 7576992.
13. Tanaka T, Kohno H, Suzuki R, Hata K, Sugie S, Niho N, Sakano K, Takahashi M, Wakabayashi K. Dextran sodium sulfate strongly promotes colorectal carcinogenesis in Apc(Min/+) mice: inflammatory stimuli by dextran sodium sulfate results in development of multiple colonic neoplasms. *Int J Cancer.* 2006 Jan 1;118(1):25-34. PubMed PMID: 16049979.

14. Al-Salihi M, Reichert E, Fitzpatrick FA. Influence of myeloperoxidase on colon tumor occurrence in inflamed versus non-inflamed colons of Apc(Min/+) mice. Redox Biol. 2015 Dec;6:218-225. doi: 10.1016/j.redox.2015.07.013. Epub 2015 Jul 29. PubMed PMID: 26262998; PubMed Central PMCID: PMC4536298.
15. Alferez DG, Ryan AJ, Goodlad RA, Wright NA, Wilkinson RW. Effects of vandetanib on adenoma formation in a dextran sodium sulphate enhanced Apc(MIN/+) mouse model. Int J Oncol. 2010 Oct;37(4):767-72. PubMed PMID: 20811697.
16. Eri RD, Adams RJ, Tran TV, Tong H, Das I, Roche DK, Oancea I, Png CW, Jeffery PL, Radford-Smith GL, Cook MC, Florin TH, McGuckin MA. An intestinal epithelial defect conferring ER stress results in inflammation involving both innate and adaptive immunity. Mucosal Immunol. 2011 May;4(3):354-64. doi: 10.1038/mi.2010.74. Epub 2010 Nov 24. PubMed PMID: 21107311; PubMed Central PMCID: PMC3130192.
17. Tammariello AE, Milner JA. Mouse models for unraveling the importance of diet in colon cancer prevention. J Nutr Biochem. 2010 Feb;21(2):77-88. doi: 10.1016/j.jnutbio.2009.09.014. Review. PubMed PMID: 20122631; PubMed Central PMCID: PMC2871384.
18. Garrett WS. Cancer and the microbiota. Science. 2015 Apr 3;348(6230):80-6. doi: 10.1126/science.aaa4972. Review. PubMed PMID: 25838377; PubMed Central PMCID: PMC5535753.
19. Romier B, Schneider YJ, Larondelle Y, During A. Dietary polyphenols can modulate the intestinal inflammatory response. Nutr Rev. 2009 Jul;67(7):363-78. doi: 10.1111/j.1753-4887.2009.00210.x. Review. PubMed PMID: 19566597.
20. Chen X, Yang L, Howard OM, Oppenheim JJ. Dendritic cells as a pharmacological target of traditional Chinese medicine. Cell Mol Immunol. 2006 Dec;3(6):401-10. Review. PubMed PMID: 17257493.
21. Cai X, Fang Z, Dou J, Yu A, Zhai G. Bioavailability of quercetin: problems and promises. Curr Med Chem. 2013;20(20):2572-82. Review. PubMed PMID: 23514412.
22. Cavalcanti E, Vadrucchi E, Delvecchio FR, Addabbo F, Bettini S, Liou R, Monsurrò V, Huang AY, Pizarro TT, Santino A, Chieppa M. Administration of reconstituted polyphenol oil bodies efficiently suppresses dendritic cell inflammatory pathways and acute intestinal inflammation. PLoS One. 2014 Feb 18;9(2):e88898. doi: 10.1371/journal.pone.0088898. eCollection 2014. PubMed PMID: 24558444; PubMed Central PMCID: PMC3928302.
23. Chen MC, Chyan CL, Lee TT, Huang SH, Tzen JT. Constitution of stable artificial oil bodies with triacylglycerol, phospholipid, and caleosin. J Agric Food Chem. 2004 Jun 16;52(12):3982-7. PubMed PMID: 15186126.
24. Tzen JT, Chuang RL, Chen JC, Wu LS. Coexistence of both oleosin isoforms on the surface of seed oil bodies and their individual stabilization to the organelles. J Biochem. 1998 Feb;123(2):318-23. PubMed PMID: 9538209.
25. Butelli E, Titta L, Giorgio M, Mock HP, Matros A, Peterek S, Schijlen EG, Hall RD, Bovy AG, Luo J, Martin C. Enrichment of tomato fruit with health-promoting anthocyanins by expression of select transcription factors. Nat Biotechnol. 2008 Nov;26(11):1301-8. doi: 10.1038/nbt.1506. Epub 2008 Oct 26. PubMed PMID: 18953354.
26. Schiechl G, Bauer B, Fuss I, Lang SA, Moser C, Ruemmele P, Rose-John S, Neurath MF, Geissler EK, Schlitt HJ, Strober W, Fichtner-Feigl S. Tumor development in murine ulcerative colitis depends on MyD88 signaling of colonic F4/80+CD11b(high)Gr1(low) macrophages. J Clin Invest. 2011 May;121(5):1692-708. doi: 10.1172/JCI42540. Epub 2011 Apr 25. PubMed PMID: 21519141; PubMed Central PMCID: PMC3083803.

27. Tanaka T, Kohno H, Suzuki R, Yamada Y, Sugie S, Mori H. A novel inflammation-related mouse colon carcinogenesis model induced by azoxymethane and dextran sodium sulfate. *Cancer Sci*. 2003 Nov;94(11):965-73. PubMed PMID: 14611673.
28. Wu S, Rhee KJ, Albesiano E, Rabizadeh S, Wu X, Yen HR, Huso DL, Brancati FL, Wick E, McAllister F, Housseau F, Pardoll DM, Sears CL. A human colonic commensal promotes colon tumorigenesis via activation of T helper type 17 T cell responses. *Nat Med*. 2009 Sep;15(9):1016-22. doi: 10.1038/nm.2015. Epub 2009 Aug 23. PubMed PMID: 19701202; PubMed Central PMCID: PMC3034219.
29. Delvecchio FR, Vadrucci E, Cavalcanti E, De Santis S, Kunde D, Vacca M, Myers J, Allen F, Bianco G, Huang AY, Monsurro V, Santino A, Chieppa M. Polyphenol administration impairs T-cell proliferation by imprinting a distinct dendritic cell maturational profile. *Eur J Immunol*. 2015 Sep;45(9):2638-49. doi: 10.1002/eji.201545679. Epub 2015 Jul 15. PubMed PMID: 26096294.
30. De Santis S, Cavalcanti E, Mastronardi M, Jirillo E, Chieppa M. Nutritional Keys for Intestinal Barrier Modulation. *Front Immunol*. 2015 Dec 7;6:612. doi: 10.3389/fimmu.2015.00612. eCollection 2015. Review. PubMed PMID: 26697008; PubMed Central PMCID: PMC4670985.
31. Bettini S, Vergara D, Bonsegna S, Giotta L, Toto C, et al. Efficient stabilization of natural curcuminoids mediated by oil body encapsulation. (2013) *Rsc Advances* 3: 5422-5429.
32. D'Introno A, Paradiso A, Scoditti E, D'Amico L, De Paolis A, Carluccio MA, Nicoletti I, DeGara L, Santino A, Giovinazzo G. Antioxidant and anti-inflammatory properties of tomato fruits synthesizing different amounts of stilbenes. *Plant Biotechnol J*. 2009 Jun;7(5):422-9. doi: 10.1111/j.1467-7652.2009.00409.x. PubMed PMID: 19490505.
33. Flemer B, Lynch DB, Brown JM, Jeffery IB, Ryan FJ, Claesson MJ, O'Riordain M, Shanahan F, O'Toole PW. Tumour-associated and non-tumour-associated microbiota in colorectal cancer. *Gut*. 2017 Apr;66(4):633-643. doi: 10.1136/gutjnl-2015-309595. Epub 2016 Mar 18. PubMed PMID: 26992426; PubMed Central PMCID: PMC5529966.
34. Manach C, Scalbert A, Morand C, Rémésy C, Jiménez L. Polyphenols: food sources and bioavailability. *Am J Clin Nutr*. 2004 May;79(5):727-47. Review. PubMed PMID: 15113710.
35. Cuttillo F, DellaGreca M, Gionti M, Previtera L, Zarrelli A. Phenols and lignans from *Chenopodium album*. *Phytochem Anal*. 2006 Sep-Oct;17(5):344-9. PubMed PMID: 17019936.
36. Pandey KB, Rizvi SI. Plant polyphenols as dietary antioxidants in human health and disease. *Oxid Med Cell Longev*. 2009 Nov-Dec;2(5):270-8. doi: 10.4161/oxim.2.5.9498. Review. PubMed PMID: 20716914; PubMed Central PMCID: PMC2835915.
37. Calixto JB, Campos MM, Otuki MF, Santos AR. Anti-inflammatory compounds of plant origin. Part II. modulation of pro-inflammatory cytokines, chemokines and adhesion molecules. *Planta Med*. 2004 Feb;70(2):93-103. Review. PubMed PMID: 14994184.
38. Sarkar S, Mazumder S, Saha SJ, Bandyopadhyay U. Management of Inflammation by Natural Polyphenols: A Comprehensive Mechanistic Update. *Curr Med Chem*. 2016 May 27;23(16):1657-95. Review. PubMed PMID: 27087243.
39. Ruby AJ, Kuttan G, Babu KD, Rajasekharan KN, Kuttan R. Anti-tumour and antioxidant activity of natural curcuminoids. *Cancer Lett*. 1995 Jul 20;94(1):79-83. PubMed PMID: 7621448.
40. De Santis S, Kunde D, Serino G, Galleggiante V, Caruso ML, Mastronardi M, Cavalcanti E, Ranson N, Pinto A, Campiglia P, Santino A, Eri R, Chieppa M. Secretory

- leukoprotease inhibitor is required for efficient quercetin-mediated suppression of TNF α secretion. *Oncotarget*. 2016 Nov 15;7(46):75800-75809. doi: 10.18632/oncotarget.12415. PubMed PMID: 27716626; PubMed Central PMCID: PMC5342779.
41. Cairo G, Recalcati S, Mantovani A, Locati M. Iron trafficking and metabolism in macrophages: contribution to the polarized phenotype. *Trends Immunol*. 2011 Jun;32(6):241-7. doi: 10.1016/j.it.2011.03.007. Epub 2011 Apr 21. PubMed PMID: 21514223.
 42. Galleggiante V, De Santis S, Cavalcanti E, Scarano A, De Benedictis M, Serino G, Caruso ML, Mastronardi M, Pinto A, Campiglia P, Kunde D, Santino A, Chieppa M. Dendritic Cells Modulate Iron Homeostasis and Inflammatory Abilities Following Quercetin Exposure. *Curr Pharm Des*. 2017;23(14):2139-2146. doi: 10.2174/1381612823666170112125355. PubMed PMID: 28079005.
 43. Raymond KN, Dertz EA, Kim SS. Enterobactin: an archetype for microbial iron transport. *Proc Natl Acad Sci U S A*. 2003 Apr 1;100(7):3584-8. Epub 2003 Mar 24. Review. PubMed PMID: 12655062; PubMed Central PMCID: PMC152965.
 44. Cinquin C, Le Blay G, Fliss I, Lacroix C. Immobilization of infant fecal microbiota and utilization in an in vitro colonic fermentation model. *Microb Ecol*. 2004 Jul;48(1):128-38. Epub 2004 Apr 19. PubMed PMID: 15085302.
 45. Dostal A, Fehlbaum S, Chassard C, Zimmermann MB, Lacroix C. Low iron availability in continuous in vitro colonic fermentations induces strong dysbiosis of the child gut microbial consortium and a decrease in main metabolites. *FEMS Microbiol Ecol*. 2013 Jan;83(1):161-75. doi: 10.1111/j.1574-6941.2012.01461.x. Epub 2012 Aug 28. PubMed PMID: 22845175; PubMed Central PMCID: PMC3511601.
 46. Dostal A, Lacroix C, Pham VT, Zimmermann MB, Del'homme C, Bernalier-Donadille A, Chassard C. Iron supplementation promotes gut microbiota metabolic activity but not colitis markers in human gut microbiota-associated rats. *Br J Nutr*. 2014 Jun 28;111(12):2135-45. doi: 10.1017/S000711451400021X. Epub 2014 Feb 21. PubMed PMID: 24555487.
 47. Scarano A, Butelli E, De Santis S, Cavalcanti E, Hill L, De Angelis M, Giovinazzo G, Chieppa M, Martin C, Santino A. Combined Dietary Anthocyanins, Flavonols, and Stilbenoids Alleviate Inflammatory Bowel Disease Symptoms in Mice. *Front Nutr*. 2018 Jan 24;4:75. doi: 10.3389/fnut.2017.00075. eCollection 2017. PubMed PMID: 29473042; PubMed Central PMCID: PMC5810255.
 48. Liso M, De Santis S, Scarano A, Verna G, Dicarlo M, Galleggiante V, Campiglia P, Mastronardi M, Lippolis A, Vacca M, Sobolewski A, Serino G, Butelli E, De Angelis M, Martin C, Santino A, Chieppa M. A Bronze-Tomato Enriched Diet Affects the Intestinal Microbiome under Homeostatic and Inflammatory Conditions. *Nutrients*. 2018 Dec 2;10(12). pii: E1862. doi: 10.3390/nu10121862. PubMed PMID: 30513801; PubMed Central PMCID: PMC6315348.
 49. De Santis S, Galleggiante V, Scandiffio L, Liso M, Sommella E, Sobolewski A, Spilotro V, Pinto A, Campiglia P, Serino G, Santino A, Notarnicola M, Chieppa M. Secretory Leukoprotease Inhibitor (Slpi) Expression Is Required for Educating Murine Dendritic Cells Inflammatory Response Following Quercetin Exposure. *Nutrients*. 2017 Jul 6;9(7). pii: E706. doi: 10.3390/nu9070706. PubMed PMID: 28684695; PubMed Central PMCID: PMC5537821.
 50. Lane ER, Zisman TL, Suskind DL. The microbiota in inflammatory bowel disease: current and therapeutic insights. *J Inflamm Res*. 2017 Jun 10;10:63-73. doi: 10.2147/JIR.S116088. eCollection 2017. Review. PubMed PMID: 28652796; PubMed Central PMCID: PMC5473501.
 51. Chen WX, Ren LH, Shi RH. Enteric microbiota leads to new therapeutic strategies for ulcerative colitis. *World J Gastroenterol*. 2014 Nov 14;20(42):15657-63. doi:

10.3748/wjg.v20.i42.15657. Review. PubMed PMID: 25400449; PubMed Central PMCID: PMC4229530.

52. Okayasu I, Ohkusa T, Kajjura K, Kanno J, Sakamoto S. Promotion of colorectal neoplasia in experimental murine ulcerative colitis. Gut. 1996 Jul;39(1):87-92. PubMed PMID: 8881816; PubMed Central PMCID: PMC1383238.
53. Grivennikov SI, Greten FR, Karin M. Immunity, inflammation, and cancer. Cell. 2010 Mar 19;140(6):883-99. doi: 10.1016/j.cell.2010.01.025. Review. PubMed PMID: 20303878; PubMed Central PMCID: PMC2866629.
54. De Santis S, Kunde D, Galleggiante V, Liso M, Scandiffio L, Serino G, Pinto A, Campiglia P, Sorrentino R, Cavalcanti E, Santino A, Caruso ML, Eri R, Chieppa M. TNF α deficiency results in increased IL-1 β in an early onset of spontaneous murine colitis. Cell Death Dis. 2017 Aug 10;8(8):e2993. doi: 10.1038/cddis.2017.397. PubMed PMID: 28796256; PubMed Central PMCID: PMC5596580.
55. Rescigno M, Chieppa M. Gut-level decisions in peace and war. Nat Med. 2005 Mar;11(3):254-5. PubMed PMID: 15746935.
56. Rimoldi M, Chieppa M, Salucci V, Avogadri F, Sonzogni A, Sampietro GM, Nespoli A, Viale G, Allavena P, Rescigno M. Intestinal immune homeostasis is regulated by the crosstalk between epithelial cells and dendritic cells. Nat Immunol. 2005 May;6(5):507-14. Epub 2005 Apr 10. Erratum in: Nat Immunol. 2015 Mar;16(3):326. PubMed PMID: 15821737.
57. Rimoldi M, Chieppa M, Larghi P, Vulcano M, Allavena P, Rescigno M. Monocyte-derived dendritic cells activated by bacteria or by bacteria-stimulated epithelial cells are functionally different. Blood. 2005 Oct 15;106(8):2818-26. Epub 2005 Jul 19. PubMed PMID: 16030185.
58. Chieppa M, Rescigno M, Huang AY, Germain RN. Dynamic imaging of dendritic cell extension into the small bowel lumen in response to epithelial cell TLR engagement. J Exp Med. 2006 Dec 25;203(13):2841-52. Epub 2006 Dec 4. PubMed PMID: 17145958; PubMed Central PMCID: PMC2118178.
59. Rescigno M, Lopatin U, Chieppa M. Interactions among dendritic cells, macrophages, and epithelial cells in the gut: implications for immune tolerance. Curr Opin Immunol. 2008 Dec;20(6):669-75. doi: 10.1016/j.coi.2008.09.007. Epub 2008 Oct 22. Review. PubMed PMID: 18852045.
60. Matteoli G, Mazzini E, Iliev ID, Mileti E, Fallarino F, Puccetti P, Chieppa M, Rescigno M. Gut CD103+ dendritic cells express indoleamine 2,3-dioxygenase which influences T regulatory/T effector cell balance and oral tolerance induction. Gut. 2010 May;59(5):595-604. doi: 10.1136/gut.2009.185108. PubMed PMID: 20427394.
61. Wehkamp J, Schmid M, Stange EF. Defensins and other antimicrobial peptides in inflammatory bowel disease. Curr Opin Gastroenterol. 2007 Jul;23(4):370-8. Review. PubMed PMID: 17545771.
62. Morel I, Lescoat G, Cillard P, Cillard J. Role of flavonoids and iron chelation in antioxidant action. Methods Enzymol. 1994;234:437-43. PubMed PMID: 7808316.
63. Xiao L, Luo G, Tang Y, Yao P. Quercetin and iron metabolism: What we know and what we need to know. Food Chem Toxicol. 2018 Apr;114:190-203. doi: 10.1016/j.fct.2018.02.022. Epub 2018 Feb 10. Review. PubMed PMID: 29432835.
64. Chieppa M, Galleggiante V, Serino G, Massaro M, Santino A. Iron Chelators Dictate Immune Cells Inflammatory Ability: Potential Adjuvant Therapy for IBD. Curr Pharm Des. 2017;23(16):2289-2298. doi: 10.2174/1381612823666170215143541. Review. PubMed PMID: 28215151.
65. Chieppa M, Giannelli G. Immune Cells and Microbiota Response to Iron Starvation. Front Med (Lausanne). 2018 Apr 18;5:109. doi: 10.3389/fmed.2018.00109. eCollection 2018. PubMed PMID: 29721497; PubMed Central PMCID: PMC5915481.